LPCSB: A Device to Distinguish Between Natural and Artificial Light

---

A Thesis

Presented to

the faculty of the School of Engineering and Applied Science

University of Virginia

---

in partial fulfillment
of the requirements for the degree

Master of Science

by

Alexander George Sarris

May 2020

APPROVAL SHEET

This Thesis
is submitted in partial fulfillment of the requirements
for the degree of
Master of Science

Author Signature: ______________________

This Thesis has been read and approved by the examining committee:

Advisor: Bradford Campbell

Committee Member: Joanne Dugan

Committee Member: Seongkook Heo

Committee Member: ______________________

Committee Member: ______________________

Committee Member: ______________________

Accepted for the School of Engineering and Applied Science:

Craig H. Benson, School of Engineering and Applied Science

May 2020

Abstract

Studies have shown that natural lighting (sunlight) is very beneficial for office workers' productivity and morale. While many new office spaces are being designed to emphasize the use of natural lighting over artificial lighting, it is difficult to determine whether sunlight actually illuminates the majority of such a workspace during the day. We present the initial results of our work in developing a new small, low-power, and wireless system that can distinguish between natural and artificial light. Previous works focus on analyzing measured light in the frequency domain. Our system analyzes light in the visible spectrum, utilizing an off-the-shelf RGB photodiode array that measures incoming light in conjunction with an algorithm that classifies the light into one of five categories – "Incandescent", "Fluorescent", "LED", "Sunlight", and "Unknown" – based on various characteristics derived from analyzing the measured components of the raw data in the visible spectrum of light (red, green, and blue). Initial testing has shown the classification algorithm to be very effective. The algorithm can correctly identify all of our tested artificial light sources with over 80 % percent accuracy and natural light with over 75 % accuracy.

To my family and my friends

Acknowledgements

It is with much gratitude that I acknowledge the help and support of my advisor, Professor Brad Campbell. His guidance and willingness to answer questions led me in many directions that I otherwise would not have considered, teaching me a lot about myself in the process.

I would like to thank my mother, the strongest person I know, who has been one of the greatest influences in how I live my life. Without her, I would be a very different person from who I am today.

I would also like to thank the members of my defense committee - Prof. Joanne Dugan and Prof. Seongkook Heo - for helping and supporting me along the way. The way that they care about their work is very inspiring and is an example for everyone to follow.

Thank you to my friends and colleagues Alan, Brenda, Will, Hussain, Jacob, Ishika, Chris, Sid, Krishna, and Varundev for all of the long and interesting conversations about various topics engineering-related and otherwise while we were either working in the Link Lab or having lunch together. I also thank all of my friends for the wonderful times that we spent together outside of the lab exploring new restaurants or at board game nights.

And finally, thank you to my research group members, friends, and colleagues Cynthia, Wenpeng, Nabeel, Rabbi, and Samyukta. You guys are all a pleasure to work with and have made life much more interesting.

This material is based upon work supported by the National Science Foundation under Grant No. 1823325.

Table of Contents

List of Tables

List of Figures

Acronyms

AC alternating current. 7

ADC analog-to-digital converter. 13, 23, 24

AI Artificial Intelligence. 6

BLE Bluetooth Low Energy. 17, 20, 22, 23, 26

CCT correlated color temperature. 24

DC direct current. 7, 8

GA Genetic Algorithm. 6

hex hexadecimal. 23, 24

I2C Inter-Integrated Circuit. 12, 13, 18, 19, 23

IDE Integrated Development Environment. 14

IoT Internet of Things. 17, 46

IR infrared. 12, 13

LED Light Emitting Diode. 2, 4, 5, 8, 9, 12, 13, 15, 18, 20–22, 25, 28, 34–37, 45, 46

LEED ID + C Leadership in Environmental and Energy Design for Interior Design and Construction. 1

LPCSB Low Power Color Sensing Board. 17, 19–21, 23, 26, 27, 29, 30, 33, 36, 37, 40, 44–49

LSB least significant bit. 23

lux luminous intensity. xi, 2, 6, 7, 15, 16, 24, 26, 46

MOSFET Metal Oxide Semiconducting Field Effect Transistor. 18

NREL National Renewable Energy Laboratory. 45

PCB Printed Circuit Board. 17, 20–22

RGB Red Green Blue. 12, 24, 27

RMS Root Mean Square. 6

RSSI Received Signal Strength Indicator. 27

SD Secure Digital. 14, 15

SoC System on a Chip. 17

STFT Short-term Fourier Transform. 8

TV television. 14

USB Universal Serial Bus. 14, 20, 21, 46

UV Ultraviolet. 2, 4

UVA University of Virginia. 5, 37, 45

XYZ CIE 1931 XYZ color space. 24

Chapter 1

Introduction

1.1 Background

1.1.1 Overview

Workplace design affects worker productivity, happiness, and health, and modern workspace design considers noise, lighting, expected tasks, and other factors when designing office spaces [1], [2]. However, this design is necessarily speculative; it must happen before the space is occupied and used. How can workplace designs be evaluated to measure how effective they are? With lighting, for example, is the office being mainly lit by the daylight entering through the windows, or are artificial lights still the main source of illumination? Research conducted in this area has shown major benefits of daylight in office spaces to workers' satisfaction and productivity [2, 3, 4, 5, 6, 7, 8, 9, 10, 11, 12, 13], but how much daylight actually illuminates the office space? Today, the amount of natural daylight illuminating an office space is one of many factors considered in the Leadership in Environmental and Energy Design for Interior Design and Construction (LEED ID + C) Certification Standards for Indoor Environmental Quality, which are used by designers all over the world to develop high-quality indoor environments as those that "enhance productivity, decrease absenteeism, improve the building's value, and reduce liability for building designers and owners" [14, 15]. However, two of the verification methods used to ensure an indoor environment's illumination by daylight rely on computer simulations of either the environment to calculate the amount of time that daylight levels are above a certain threshold, or the level of daylight intensity between 9:00am and 3:00pm [15]. A third verification method relies on physical measurements of the daylight intensity in said indoor environment [15]. It is unclear how daylight is distinguished from artificial light unless the measurements require that all artificial light sources are deactivated, which would imply that the verification relies on the absence of artificial light while measuring sunlight and cannot distinguish between the two. This work focuses on windows and daylight exposure in the context of determining how much of the light illuminating a workspace is actually natural daylight vs. how much is artificial (Light Emitting Diode (LED), fluorescent, or incandescent) through physical measurements instead of simulations.

1.1.2 Existing Devices

There are a number of existing devices on the market that could be used to identify different types of light. Existing ultraviolet sensors measure the levels of Ultraviolet (UV) A-type, B-type, and C-type radiation in an environment, and are most often used to detect when the levels are concentrated enough to be harmful to humans [16]. These could be used to identify sunlight because sunlight contains UV light, but identifying sunlight is not a primary function. These sensors could also be used to identify fluorescent light, since some types of compact fluorescent lights do emit potentially strong levels of UV radiation through cracks or defects in their internal phosphor coating [17]. There are ambient light sensors in devices such as smartphones or smart lighting systems that are used to measure the amount of light in an environment and adjust the brightness of the light emitted by the device(s) accordingly [18]. There are other sensors that use light to help determine the color of a nearby object [19], measure blood pressure and heartrate [20], and even calculate distance from a target [21]. There are also sensors that are able to measure incident light and output a square wave in response. These sensors could be used to distinguish between certain types of light, but seem to be designed for use in areas involving the measurement of luminous intensity (lux) [22].

1.2 Thesis Overview

However, none of these devices have the capability to distinguish between all types of artificial light (LED, Fluorescent, and Incandescent) and natural daylight. A device able to do this could provide a much-needed tool that would allow building designers to be more precise when placing various features meant to emphasize natural lighting, give office workers the ability to tell when their environment is being lit by daylight or artificial light and adjust their environment accordingly, or even allow an automated environmental monitoring system to do the same thing. Such a device would need to be small, low-power, able to be placed on any surface, and capable of continuously monitoring the lighting in high-resolution across an office space. This would enable the evaluation of whether the workspace design matched its designers' goals and simulations, better tracking of energy consumption based on artificial lighting use, and understanding the lighting preferences of specific occupants to improve the work environment for everyone.

We present the initial results of our work in developing a new method for using an RGB color sensor in conjunction with a data-processing algorithm that allows for the identification of the dominant type of light illuminating an environment. We argue that different types of light (incandescent, fluorescent, LED, and sunlight) have noticeable differences in their RGB color spectra and that these distinctions can be measured and identified in enough detail to allow for the identification of the dominant light source in question without more complicated equipment. Our setup includes a small, off-the-shelf RGB photodiode array mounted on a printed circuit board (PCB) roughly 24mm x 39.5mm in size and an algorithm that classifies measured light based on analysis of its red, green, and blue components of the visible spectrum of light. With all identification tests run, the classification algorithm was able to identify incandescent light 100 % of the time, fluorescent light 82 % percent of the time, LED light 81 % percent of the time, and sunlight 77 % percent of the time.

1.3 Use Cases

1.3.1 Increasing Productivity

A system that can identify the type of light illuminating an environment could be very useful in a number of cases. The primary instance that we focused on in this work involves measuring lighting in an office workspace. As stated earlier, many studies have been conducted that show how natural lighting (sunlight) improves office workers' morale, productivity, and overall sense of well-being [2, 3, 4, 5, 6, 7, 8, 9, 10, 11, 12]. While many new workspaces are being designed to emphasize natural lighting throughout themselves, it is very hard to fully test the design during construction. While it is obvious that designers can easily run simulations of various environmental conditions of a workplace using modern technology, it is very difficult to account for every possible action that the workers using the space can take. Furniture could be moved, windows could be closed or blocked, and the workplace in question could be used in many different scenarios other than what it was designed for. A light-identification system deployed in a workspace would be extremely useful, able to help designers understand if and how natural light is reaching all of the areas in the workspace that were designed to allow for it.

1.3.2 Energy Management

Another application in which a system for identifying light could be very useful is in energy management. In many buildings, lights are often left on in certain areas when nobody is working there, which is wasting electricity that could be used elsewhere. Some buildings do have motion sensors installed that turn on the lights when movement is detected, but these do not record the exact time that the lights are turned on unless the motion sensors are also connected to an alarm system. The time that the lights turn off again is not recorded either. While monitoring what specific lights are active at specific times would be useful in determining how lighting consumes electricity in detail, installing a system connected to each light source that could do so would be very expensive and cost-prohibitive. Installing a non-invasive sensor network that could measure and identify the type of light illuminating a space would be more useful, showing when people are turning lights on or off at any point throughout the day. While it wouldn't be as precise as measuring the energy consumption of individual light sources, identifying the type of light illuminating a space could allow one to estimate the efficiency of the light source (LED vs. incandescent) and use that in conjunction with other devices to figure out which sections of a building use the most energy.

1.3.3 Personalizing a Space

Another area where a light-identification system could be very useful involves making spaces more personal, work-related or otherwise. Many people have different lighting preferences, but workspaces often use a single type of light throughout. A light-identification system could be used to automatically measure what kinds of light are illuminating a workspace, allowing people to know what type of lighting they are working in, how intense the lighting is, and adjust their space accordingly. While many of the sensors described earlier can be used measure the intensity of light in a workspace, to our knowledge there are no similar devices designed to be used in a workspace that can also identify the type of light illuminating it.

1.3.4 Medical Applications

A light-identification system could also be useful in medical applications involving light exposure. Sunlight (specifically the UV-B component) is instrumental in getting the human body to produce vitamin D, but vitamin D deficiencies are very common in the United States, which exacerbates a host of health concerns in response [23]. A small wearable light-identification system could be very useful to people with Vitamin D deficiencies if they choose to expose themselves to sunlight to increase their Vitamin D production instead of taking Vitamin D supplements. However, this use case may not be one of the main options for a light-identification system because many doctors recommend "avoiding sunlight and getting Vitamin D by mouth" [23].

1.4 Test Environment

The Link Lab is a recently constructed laboratory on the second floor of Olsson Hall at the University of Virginia (UVA), designed to prioritize natural daylight over artificial lighting. It houses over 250 graduate students and faculty who work in various departments, and conducts research in Smart Cities, Smart Health, and Autonomous Vehicles and Robotics [24]. The office space where the majority of the students and faculty work is wide open, with the students' desks placed next to each other in multiple rows. The office space is divided into two sections by a central hallway and three conference rooms distributed evenly along one side of the hallway. The faculty offices are placed in one of the resulting sections such that all offices have at least one window, and they are separated from the rest of the office section by glass walls to allow as much natural light to fall in the student work area as possible. For the other section of the office space (where there are no faculty offices), there are large windows spaced at regular intervals to allow more natural light into the work environment. The lab also has artificial lighting consisting of LED ceiling lights meant to be used in the instances where the workspaces are not adequately lit by sunlight, as well as motion sensors in the ceiling that turn on the ceiling lights when the sensors detect movement. The Link Lab is being used as the initial test environment for the work described in this paper, with plans to test additional areas in nearby buildings and add a unique new environmental analysis method to the lab's network if promising results are obtained.

Chapter 2

Related Works

2.1 Artificial Intelligence (AI)

Differentiating between natural light (sunlight) and artificial light has been examined in other contexts indirectly related to increasing workers' daylight exposure and improving morale. They mainly center around energy monitoring using various techniques. Coley and Crabb (1997) approached the problem using Artificial Intelligence (AI). They tested the application of a "Genetic Algorithm (GA)", a type of algorithm that "can handle non-linear, ill-defined problems of many dimensions in search spaces with many local minima and are capable of processing large quantities of noisy data efficiency" [25] in an application that is "capable of the real-time prediction of natural light levels at chosen points within a room using external measurements of vertical plane illuminance" [25]. Their setup involved a series of photocells (one placed in a room near the ceiling and five placed on the roof of the same building) to estimate the amount of natural light illuminating the room from light levels outside the building. Their method was very accurate – "within a Root Mean Square (RMS) error of 3 % at an illuminance of 500 lux" [25] – in identifying artificial light vs. natural light, which is very useful in determining whether artificial lights are being used. However, it does not appear to distinguish between different types of artificial light, which would keep it from working well in more detailed energy-management applications. In these applications, the goal is not just to distinguish whether natural or artificial light are illuminating in an environment, but also to figure out how much energy the artificial light sources are consuming; different types of artificial light sources consume different amounts of energy.

2.2 Controlling Color Temperature

Another group didn't focus specifically on identifying types of light, but did touch on it to some degree in their work. Their research involved controlling the artificial light being emitted into an environment. Begemann et al. (1998) developed and patented a device to control the color temperature of an artificial lighting system. This device measures the intensity of natural daylight incident on a desk and adjusts the color temperature of a connected lighting system accordingly [26]. The patent describes the device's method of operation in great detail and discusses the results of a study conducted by the developers, in which participants worked in an office space that had the color-temperature-controlling device installed, allowing the user to adjust both the color temperature and intensity of the artificial light. The researchers found out that people would mostly ignore adjusting the luminous intensity (lux) of the light, but enjoyed adjusting the color temperature of the light to better suit their preferences [26]. While not actually focused on differentiating between artificial and natural light itself, this work does provide insight into one of several potential variables that could be useful in doing so. This method would be very useful in personalizing one's workspace, but would not be as helpful in energy management applications or workspace lighting evaluation.

2.3 Frequency Domain

Fassbender et al. (2010) took a different approach to identifying light. They developed and patented a handheld device meant to "distinguish artificial light from sunlight and low-frequency artificial light from high-frequency artificial light" [27]. The device is described as only working with light sources that are either powered by an alternating current (AC) source or include magnetic or electronic ballasts; it will not work with lights powered by direct current (DC) sources [27]. It consists of a photodetector, amplifier, two filters, and an indicator that displays what type of light was measured [27]. Unfortunately, while the patent does describe the device's method of operation in great detail, it does not cover any results from tests conducted with the device, leaving it unclear as to how well the device actually works. However, it does raise the possibility of measuring the frequency / modulation of the light as a promising approach to identifying types of light. Because the device is handheld, it would be very useful in conducting an immediate evaluation of an office space in terms of measuring natural lighting or energy management, but would be less suitable for long-term analysis.

Jazizadeh and Wang (2016) approached the problem of distinguishing between natural and artificial light using a combination of the methods from both Coley and Grabb (1997) and Fassbender et al. (2010). Their objective was to develop a method to monitor the energy consumption of a lighting system using "single light intensity sensors" [28]. Their setup used photodiodes to measure ambient light in a manner similar to Coley and Grabb. Unlike Coley and Grabb, they used only one photodiode placed on a table 60 cm above the floor instead of near the ceiling. Similar to Fassbender et al. (2010), Jazizadeh and Wang (2016) analyzed the frequency of the incident light to try identifying it. Unlike Fassbender et al. (2010), they used a Short-term Fourier Transform (STFT) instead of two filters to do this, demonstrating that fluorescent light has distinguishing characteristics in the frequency domain at specific harmonics, and that measuring in the frequency domain does appear to be a viable approach to identifying fluorescent light [28]. However, it is unclear from their work how well this approach will work with incandescent or LED light sources, and, similar to Fassbender et al. (2010), it is unclear how well the approach will work with DC artificial light sources because the fluorescent bulbs used by Jazizadeh and Wang (2016) utilize a ballast to regulate the flow of current through them [28]. This approach could be useful in long-term evaluation of an office space in terms of natural lighting or energy management, as well as in a wearable device meant to measure sunlight levels. However, Fourier Transforms are computationally intensive, and it is unclear if this approach would be suitable for applications requiring a low energy consumption.

2.4 Summary

Our approach to distinguishing between natural and artificial light relies on a more detailed analysis of the light measured by a series of photodiodes. Instead of measuring the intensity of light or analyzing collected data in the frequency domain, we look to elements of the visible spectrum. These elements are present in all types of light, regardless of whether they are natural or artificial in nature.

Chapter 3

Requirements

3.1 Classification Accuracy

Before building our proof-of-concept light-identification system, we first needed to identify what the main requirements of a light-identification system would be. Some of these requirements could vary based on the specific use case of the system, but there are several main requirements that we believe should be addressed regardless of the use case. The first is "accuracy of classification". We believe that this requirement is the most important, because there is no reason to build a system meant to identify light using a specific method if the method in question doesn't work. By "accuracy of identification", we mean the ability of the system to correctly classify measured light as "Incandescent", "Fluorescent", "LED", or "Sunlight".

For this work, our primary goal was to demonstrate the "accuracy of classification" of the light-identifying system and show that all measured light could be classified correctly over 75 % of the time. An accuracy of at least 75 %, a clear majority for an untested concept, would show that the concept has potential and should be further refined and explored. If the system is not accurate for a majority of the time, then that implies that the approach needs to be reconsidered.

3.2 Wireless Data Transmission

Another requirement of a light-identification system that could be important is the ability to transmit data wirelessly, although this depends on the specific application of the system. If such a system is installed in an office workspace, transmitting data wirelessly would make it much easier for the user(s) to analyze the measurements from the various light-measuring sensors distributed around the environment and generate a clear picture of how the environment is illuminated. If the sensors were not wireless, then they would either have to be physically connected to a central hub responsible for analyzing the collected data, or the data would have to be stored locally on the measuring device and be physically retrieved and transported to the location where the data is analyzed. Neither of these options would be cost effective nor efficient. Ideally, the measurement devices would be able to transmit data over a range of 5-15 feet, depending on the size of the space and whether it is intended to house only one person or be a communal workspace for several people. This also assumes that the unit processing the transmitted data is located near the center of the workspace to reduce the maximum distance that the measurement device(s) need to transmit. However, if the light-identification system is implemented as a handheld or wearable device, then wireless transmission would not have to be required –the device could be transported around an environment and identify the illuminating light when commanded to do so.

We also tried to meet the “wireless data transmission” requirement to some degree, such that our proof-of-concept device could potentially be used in use cases similar to the office-monitoring scenarios or the wearable light-monitoring system described above. In this project, “wireless data transmission” means that a measuring device in the light-identifying system is able to successfully send data from itself to a receiving device without any physical connection between the two.

3.3 Mobility

A third requirement that could be important for a light-identification system is mobility. A system meant to be implemented in an already-existing work environment should be unobtrusive, easy to install, and not interfere with regular operations. By this requirement, if the system involves multiple measuring devices, it also makes sense for the devices in question to be small, light, and adaptable, able to be placed in any location (such as an office environment or a manufacturing facility) depending on the layout of the environment in which it is deployed. If these requirements are met, then this system should have only a low chance of disturbing regular workers and causing them to deviate from their normal routine. Mobility is also important for light-monitoring wearable devices, such as such as a sunlight-monitoring bracelet to track sunlight exposure for someone with a vitamin D deficiency. For wearable devices, the focus for mobility is on size, weight, and ease of use. They should be slim, light, and not cause discomfort when worn.

For mobility, we chose to make the measuring device small and light to facilitate easy deployment while using a central receiving station to process all transmitted data for easier analysis. In this work, the main limitation to mobility was the receiving station that processed the measured data, so we chose to design the measuring device with dimensions of less than 5 cm by 3 cm to make it easier to deploy in a variety of locations around the station. The maximum distance from the station was limited by the range of the wireless transmissions from the measurement device. For identifying light in an office space, measurement devices should be distributed throughout the space and transmit data to a receiver that processes the data accordingly.

3.4 Energy Cost

The last requirement that we considered important was energy cost. We saw this requirement as most relevant in both light-monitoring applications for reducing energy consumption and in wearable technologies. In work environments, it does not make sense to have a device with high energy consumption monitoring lighting if the goal is to reducing the energy consumed in the work environment. For wearable technologies, such as the sunlight-monitoring bracelet described above, it is important that the device be worn as much as possible to keep an accurate record of the patient's light exposure, which means that the device should not run out of power when the sun is in the sky and should have to be recharged only rarely. Ideally, this means that in both of the applications described, the measurement device(s) would be powered by an energy-harvesting supply and an energy storage device. The combination of these two components would allow the device to be powered by a battery, which would be supplemented by the energy-harvesting system to allow for continuous use if the device would otherwise consume too much energy. This requirement is also indirectly related to the frequency of light measurements and data transmission – the higher the measurement frequency of light and transmission frequency of data, the more energy is consumed by the device.

We chose to meet the "low energy cost" requirement by focusing on the energy consumption of the individual components of the light-measuring device(s) used in the system. We decided to not develop an energy harvesting power supply as described above in order to focus on the accuracy of the identification system itself. A low-energy consumption implies low power, which means low voltage supplies and low current consumption. We chose to meet the "low energy cost" requirement by using components that were supplied by 5 V or less and consumed fewer than 10 mA of current. These requirements are not final and could easily be tightened in development beyond a proof-of-concept.

Chapter 4

Preliminary Feasibility Study

4.1 Overview

First, we had to determine if it would actually be possible to measure ambient light with enough precision using a small and low-cost sensor. Based on the requirements described above, we needed to build a proof-of-concept device that could consume low amounts of energy, was small in size, and composed of off-the-shelf components. We chose two sensors to test for use in this proof-of-concept: a MAX30105 breakout board sold by Sparkfun, and TCS34725 Red Green Blue (RGB) color sensor mounted on a breakout board sold by Adafruit.

4.2 Hardware Tested

4.2.1 Sensors

MAX30105

The MAX30105 particle sensor breakout board (Figure 1) consists of a small optical module, three surface-mount LEDs, and some power supply and Inter-Integrated Circuit (I2C) communication circuitry. The I2C commands come from a connected microcontroller, and the board uses the optical module to measure the reflection of the LEDs off of particles or different materials situated in front of the optical module. The three LEDs include a red LED, a green LED, and an infrared (IR) LED. According to the breakout board's datasheet [29], it is used in applications involving fire alarms and smoke detectors in areas such as building automation and mobile / wearable devices.

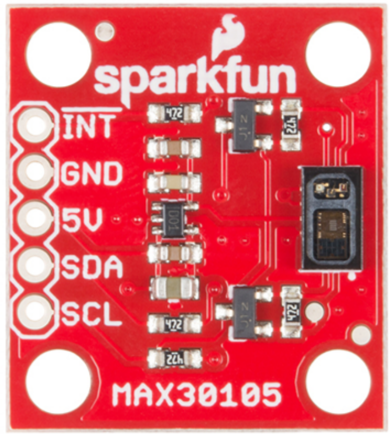

Figure 1: A MAX30105 Particle Sensor Breakout Board [20]

TCS34725

The TCS34725 color sensor breakout board (Figure 2) consists of a small LED, some power supply and I2C communication circuitry, a white LED, and the TCS34725 color sensor. As with the MAX30105 board, the TCS34725 board receives I2C commands from a connected microcontroller and sends certain information back to the microcontroller that depends on the received commands. The sensor itself consists of a 3x4 photodiode array in a compact package. In addition to an IR blocking filter that reduces the IR spectral component of detected light, each photodiode has one of several possible color filters over of it. One filter is red, another is green, a third is blue, and the fourth "filter" is clear [30]. The photodiodes in the 3x4 array are divided evenly among the filter types. Four analog-to-digital converter (ADC)'s convert the current read from the photodiodes into 16-bit values that are then sent over the I2C serial bus to a connected processor [30].

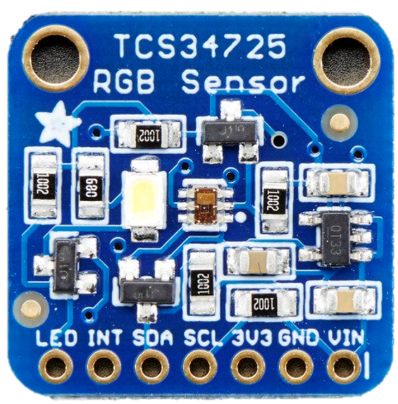

Figure 2: A TCS34725 RGB Color Sensor Breakout Board [19]

4.2.2 Processor

Tinyduino

The microcontroller used to test each of the above breakout boards is known as a "Tinyduino". The Tinyduino is designed to be as modular as possible, Arduino-compatible, and programmable using the Arduino Integrated Development Environment (IDE) [31]. It uses the Atmel ATmega328p microcontroller [32], which is shared with the standard Arduino Uno board as well. The main difference between the two boards is the size, with the Tinyduino having a form factor that's about the size of a quarter while the Arduino Uno is about the size of a credit card. Like the Arduino Uno, the Tinyduino has its own "shields" – boards that are designed to plug into the Tinyduino processor to add new sensors to interface with. We used a Tinyduino Universal Serial Bus (USB) shield to allow the processor to plug into a computer to be programmed and a television (TV) screen shield to display the data being captured. After preliminary testing, we removed the TV screen and added an Secure Digital (SD) card shield was added to save the captured data for later examination. Figure 3 shows the TinyDuino processor and the shields that were used to interface with it and the color sensor.

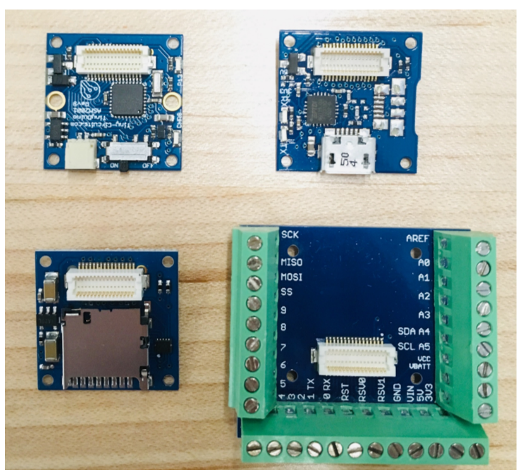

Figure 3: The Tinyduino and shields used in this work. Top row from Left to Right: Tinyduino Processor, USB Programming Shield. Bottom row from Left to Right: SD Card Shield, Prototyping board with connector terminals

We programmed the Tinyduino Processor in the Arduino IDE to make the processor interface with whichever sensor was connected to it through I2C. Its first job was to read the sensor identification number and check to see if it matched the number specified in either the MAX30105 or the TCS34725 datasheets. If the number matched with one of them, then the program had the processor calibrate the sensor and start reading data from it. After examining preliminary data from both sensors, we determined that the MAX30105 only worked well if there was an object placed directly in front of it for light to reflect off of the object to the sensor. The TCS34725 could be configured to measure ambient light and did not require an object to be placed really close to it, so we decided to use that one with this project. We used the raw data measured by the TCS34725 to calculate the color temperature and lux of the measured light and saved the results of the calculations along with the raw data to an SD card, before transferring the data to a Microsoft Excel spreadsheet and graphing it in several scatter plots.

4.3 Initial Tests

To ensure that the data was not affected by external sources, we took all measurements of artificial light sources (Incandescent, Fluorescent, LED) with the Tinyduino by placing the light source and the TCS34725 in an enclosed container, with the sensor placed 10 cm in front of the light source. We aimed the light source directly at the sensor and ran the tests for around eight hours for each light source. It was not possible to do this when measuring sunlight, so we placed the sensor on a windowsill and made sure that there were no artificial light sources nearby and that sunlight was only type of light available for those measurements. We ran the sunlight measurements for around two hours each. We repeated the above process with several different light sources, with the same variables being measured each time. Sample data from the TCS34725 and Tinyduino setup can be seen in Figures 4 and 5, showing visible differences between the attributes of Incandescent light, Fluorescent light, LED light, and sunlight. This data shows that there are very distinctive differences between different types of artificial light in not just the visible spectrum, but also in color temperature and lux.

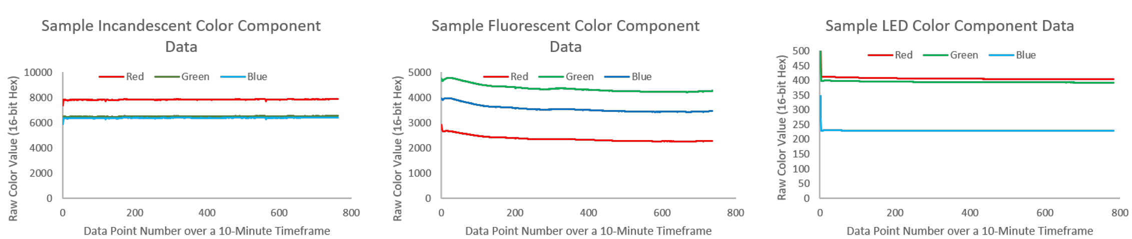

Figure 4: Sample color data from different light bulbs measured by the TCS34725 breakout board and the Tinyduino. The line colors correspond to specific filters in the photodiode array (e.g. the red line with the red-filtered photodiodes).

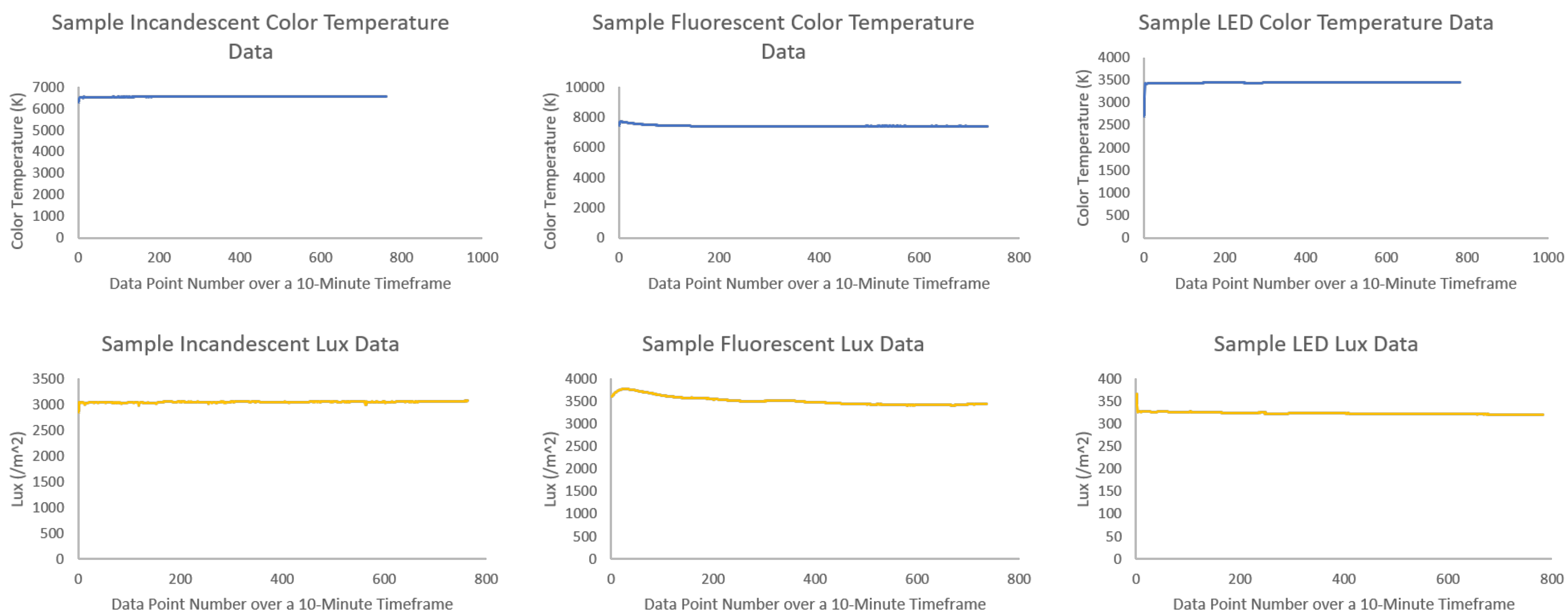

Figure 5: Color temperature and lux values calculated from the sample color data displayed in Figure 4. The data lines are relatively steady over time, but the magnitudes of each are fairly different.

Chapter 5

LPCSB Design

5.1 Hardware

5.1.1 Schematic

The original prototype was satisfactory as a proof of concept, but was not able to transmit data wirelessly and consumed too much energy to be of practical use in low-power Internet of Things (IoT) applications. For this reason, we decided to design a Printed Circuit Board (PCB) that would interface the TCS34725 sensor with a new microcontroller that would consume much less power than the Tinyduino. We named the final device the "Low Power Color Sensing Board (LPCSB)".

The TCS34725 sensor was of the same type used in the proof-of-concept device. It consumes 235 µA of current when active and only 2.5 µA when in sleep mode [30]. The selected microcontroller was the nRF51822, described as "an ultra-low power 2.4 GHz GHz wireless System on a Chip (SoC) integrating the nRF51 series 2.4 GHz GHz transceiver, a 32-bit ARM® Cortex$^{\mathrm{TM}}$-M0 CPU, flash memory, and analog and digital peripherals" in to its datasheet [33]. Circuitry to enable the transmission of data from the 2.4 GHz Bluetooth Low Energy (BLE) transceiver was also required. This processor was chosen not just because it consumes a very low amount of current when in sleep mode [33], but also because of its BLE transceiver. While BLE does allow encryption and two-way communication between connected devices, it also has an "advertising mode" that allows for one-way communication. Advertising is usually used by devices to indicate their presence and allow connections to be established between them, after which the devices in question will stop advertising [34]. However, advertising can also be used to broadcast data to any device that happens to be in range. To do this, a custom payload needs to be inserted into the advertising packet, specifically under “Manufacturer Specific Data” [34]. Using this method would allow us to avoid connection protocols, data exchanges, passwords, and other similar features needed for connected Bluetooth devices.

The reference schematic used in the LPCSB design for the nRF51822 (Figure 6) contained the processor, power supply and charging circuitry, Bluetooth transmission circuitry, a device made by DecaWave that incorporates three antennae, and circuitry for an external 16 MHz clock required to operate certain functions of the nRF51822 [35]. Figure 7 shows the reference schematic for the TCS34725, which contains the sensor, a 3.3V regulator, level-shifting circuitry so that the I2C communication can be done with either 3.3V or 5V logic, an LED, and a Metal Oxide Semiconducting Field Effect Transistor (MOSFET) driver that drives said LED [36].

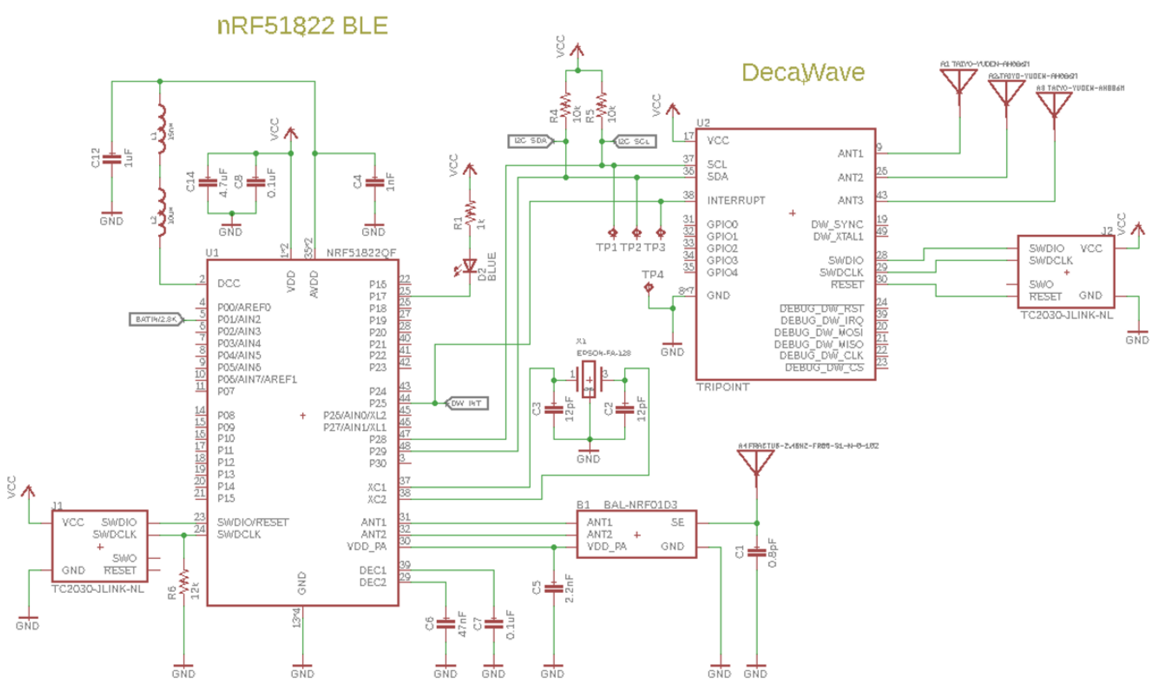

Figure 6: Reference schematic that includes the nRF51822 processor [35]

Since the LPCSB needed to consume a low amount of power and execute just a few specific functions, we realized that it was not necessary to include a large amount of the circuitry in each reference schematic because the circuits in question had their own functionality, were not required for the operation of the TCS34725 or the nRF51822, and were not needed for the LPCSB’s desired functionality. From the original TCS34725 schematic, we used only the sensor itself. The sensor operates at a default value of 3.3V [30], the same as the nRF51822 [33]. This let us eliminate the level-shifting circuitry, the LED and MOSFET driver, and the voltage regulation circuitry. From

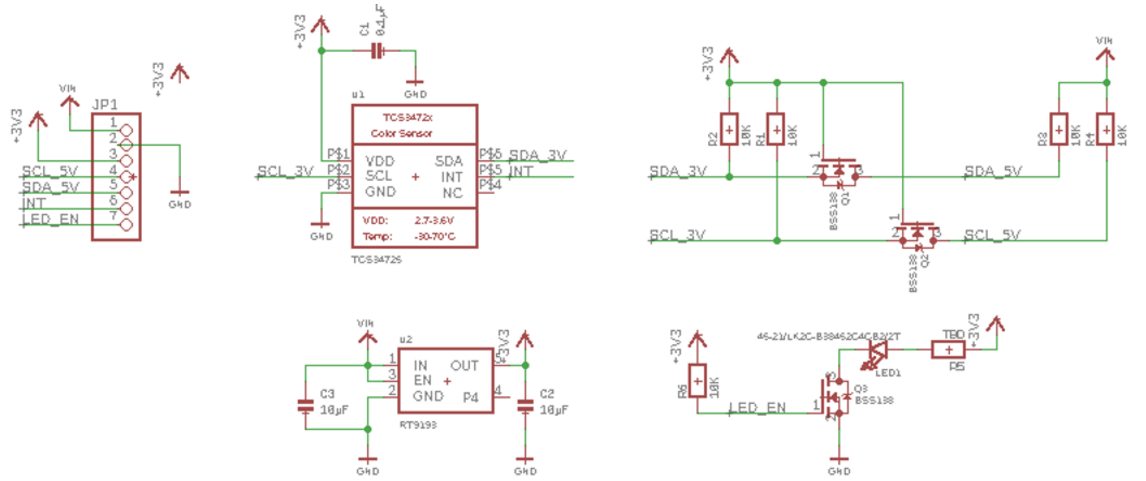

Figure 7: Reference schematic for the TCS34725 breakout board developed by Adafruit [36]

the nRF51822 schematics, we just used the nRF51822 processor, its clock circuits, its power supply connector, and its 3.3V regulation circuitry. The TCS34725's VDD pin was connected to the VCC output from the Power Supply and Charging Circuit, and its I2C communication lines were connected to the ones from the nRF51822. The final schematic for the LPCSB can be seen in Figure 8.

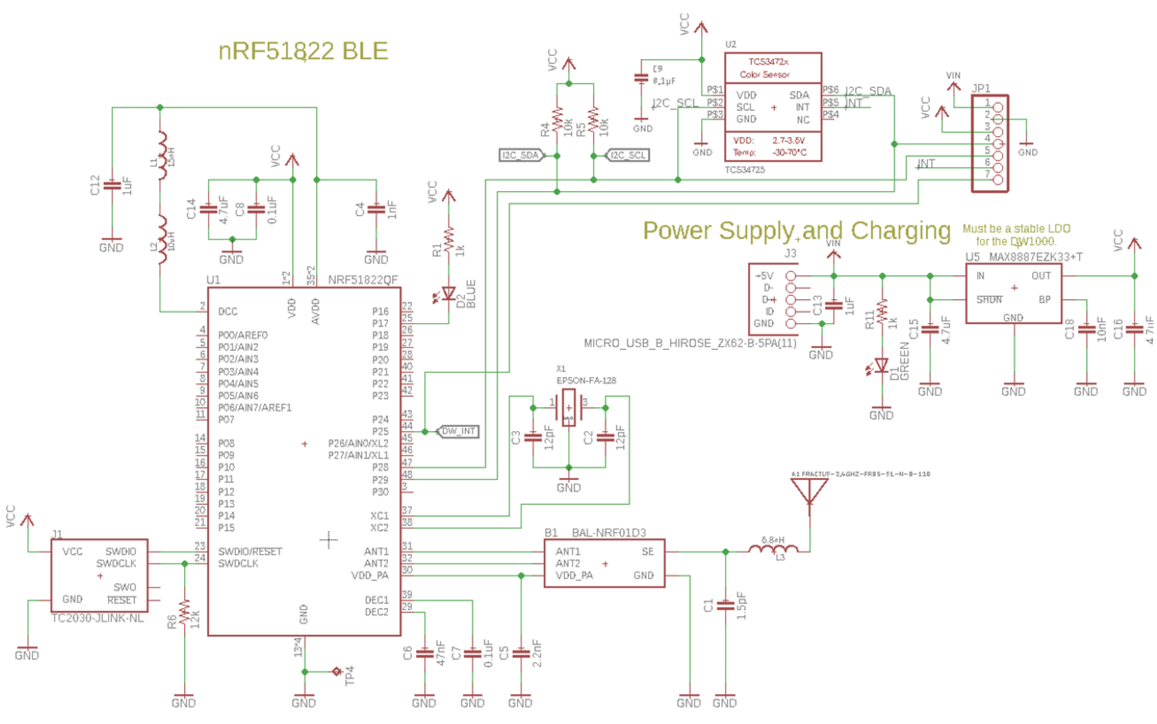

Figure 8: Final circuit schematic for the LPCSB

5.1.2 Layout and Assembly

We set up the PCB layout to make the virtual connections between components as short as possible to save space, making the final board as small as possible and able to be placed unobtrusively in various locations if desired. We started with the Micro Reach Xtend (FR05-S1-N-0-110) Chip Antenna, placing it on the edge of the PCB. According to Page 9 of its datasheet, the antenna is supposed to be placed in a "clearance area", an area of the PCB that is not connected to a Ground plane [37]. The specific dimensions referenced in this figure apply "for the reference evaluation board described on page 5 of [the antenna's datasheet]" [37]. We decided to use the dimensions specified on Page 9, because the reference board dimensions described on Page 5 were very close to the final dimensions of 2.5 cm x 3.9 cm for the LPCSB [37]. This was the only constraint on PCB dimensions. The processor was placed near the antenna clearance area to make sure that the connections between the processor, the antenna matching network specified in the datasheet, and the actual antenna were as short as possible. The USB connector and header pins were placed in corners to keep them out of the way of the other components. Components connected directly to the processor were placed near their corresponding pins on the processor to reduce the length of the connecting vias. Power supply components interfacing with both the processor and the USB connector were placed between the two for the same reason. The color sensor was placed near the header pins because the header pins were placed in a section of the PCB relatively empty of components, which would reduce the chance of any light reflecting from the other components reaching the sensor. This assumes that the header pins are not soldered onto the PCB, which was the case with the LPCSB that we used for all tests described later. Ten boards were ordered to make sure that there were backups for testing and troubleshooting. The board layout for the first iteration of the LPCSB can be seen in Figure 9.

To assemble the PCB, we used a template, solder paste, a microscope, and forceps to drop each component into its proper location. We then transferred the PCB onto a hot plate, heated it to 260 degrees Celsius, and left it at that temperature until all of the solder paste melted into pools of reflective silver liquid, which secured the components into their places on the PCB after the melted solder re-solidified. We planned to test a random board in sections: first the power regulation, then the ability interface with the processor and upload a basic "Blink" program to turn an LED circuit on and off, then the BLE Radio, and last the color sensor. LED circuits described in this paper consist of an LED connected in series with a 1 kΩ resistor. A fully assembled LPCSB can be seen in Figure 10.

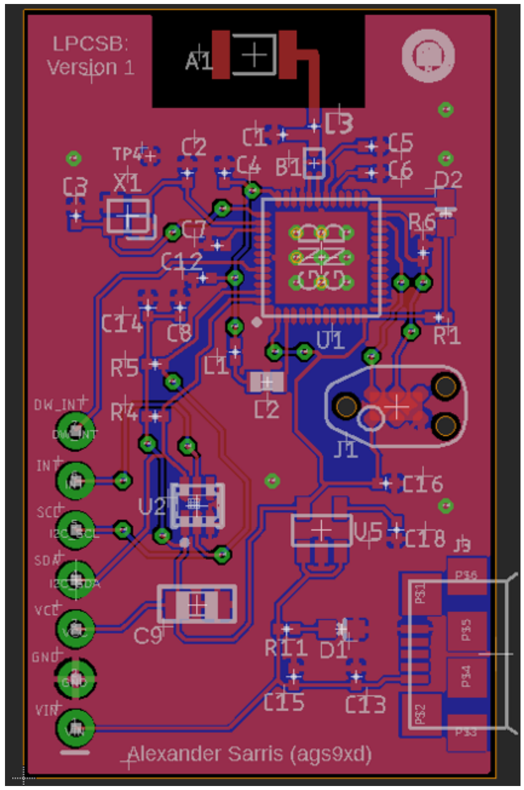

Figure 9: PCB layout for the LPCSB. The board has two layers. The top layer is shown in red and the bottom layer is shown in blue.

5.1.3 Hardware Testing

Power Regulation

The power regulation section consisted of a micro-USB B-type connector, a green LED indicator circuit, a MAX887EZK33+T Low-Dropout 300 mA 3.3 V Linear Regulator [38], and several bypass capacitors meant to help stabilize the input / output voltage and current in case of supply fluctuations. The assembled circuitry was tested through visual observation and with a multimeter. The visual observation involved looking to see if the green LED lit up when power was applied, while the multimeter was used to check if the voltage output from the regulator was the 3.3 V specified in the datasheet.

Processor

The second section of hardware tested involved the nRF51822 processor, its clock circuitry, a blue LED circuit, its connection to the 3.3 V output from the voltage regulator section, and an interface for a J-Link Segger programming interface. The test code for blinking the blue LED circuit was

Figure 10: Fully assembled LPCSB.

pulled from the “Lab11 nrf5x-base” GitHub repository [39] and modified to ensure that the pin connected to the LED circuit was the one being controlled by the code.

The third section of hardware tested included everything from the previous section, along with the BLE Radio transmitter inside the nRF51822. The transmitter was connected to a BAL-NRF01D3 transformer balun [40], the antenna described earlier, and the impedance matching network that was constructed as described in the antenna’s datasheet [37]. We uploaded a “beacon-Unicode” program from the “Lab11 nrf5x-base” GitHub repository [39] to the board and used the “LightBlue” phone application (app) to monitor any outgoing transmissions from the board. However, the application did not intercept any Bluetooth transmissions from the PCB, indicating that the BLE Radio was not working. We verified this by uploading the same program to a PCB from an unrelated research project and monitoring outgoing transmissions from it. The “LightBlue” app was able to intercept the transmissions from this new PCB. We eventually discovered that the problem was with hardware on the LPCSB: an external 26 MHz clock was connected to the nRF51822 instead of an external 16 MHz clock, and that supplying an incorrect external clock frequency to a processor can cause certain features to operate incorrectly or not operate at all. After replacing the clock, the LPCSB was able to successfully transmit data.

The final section of hardware included everything from the previous sections, along with the TCS34725 color sensor. As described earlier, the color sensor uses I2C communication to send and receive information to/from a central processor, in this case the nRF51822. To test this section of hardware, we wrote a program that would have the nRF51822 instruct the TCS34725 to measure the ambient light and send the resulting values back to it. We programmed the processor in C, using the "nrf5x-base" [39] and "Adafruit-TCS34725" GitHub repositories as design references [41]. Three code files were written: an "h" file, a "cpp" file, and a "main" file. The "cpp" and "h" file are devoted to the TCS34725 color sensor, containing only the function prototypes, global variables, and register values from the "Adafruit-TCS34725" repository that were needed for the LPCSB's desired functionality [41]. The "main" file contains code for interfacing with and controlling the TCS34725 color sensor, which consists of five steps. It also contains code to read data from the sensor and advertise the collected data over BLE.

Sensor Interface

The first step to interfacing with the TCS34725 is to activate the I2C communication lines in the nRF51822 and start one of its internal timers. When the timer expires, the next step is to ensure that the I2C channel is working properly and that there is in fact a link between the processor and the color sensor. To do this, the processor sends a command to the color sensor to read the "ID Register", which is read-only. The hexadecimal (hex) value returned from the sensor to the processor should be "0x44", as specified in the sensor datasheet [30]. The third and fourth steps is to configure the "Integration Time" and "Gain" settings for the sensor by sending 0x00 to the RGBC Timing Register (address 0x01) and 0x00 to the Control Register (address 0x0F) respectively, which sets the integration time of the sensor's ADC's to 2.4ms and the gain of the ADC to "1X" [30]. The fourth register to configure is the "Enable Register", which is responsible for enabling various functions and interrupts [30]. The hex value that should be sent from the processor to the sensor at this stage is 0x01, which is the command to activate the sensor's internal oscillator. Activating the oscillator will allow the internal hardware timers and ADC channels to be configured. The fifth step is to send the hex value 0x03. The least significant bit (LSB) ensures that the oscillator stays enabled while the second bit turns on the two-channel ADC responsible for converting the analog values read from the sensor photodiodes to the digital values that are sent to the connected microcontroller [30]. There are other settings for the sensor that were not explored in this project.

Measurements taken by the color sensor can only occur and can only be accessed after the color sensor is configured similarly to what is described above. As stated earlier, the TCS34725 contains four ADCs to interface with its photodiode array, which consists of red-filtered, green-filtered, blue-filtered, and clear (unfiltered) diodes. The data for each color is stored as a 16-bit value split between two registers. Each register can store only one value at a time, and the stored values are overwritten each time a new measurement is taken. A unique hex value is required to access each register individually. To read data for a specific color, a two-byte read operation is required. The first part of the operation reads the data from the lower byte register to a connected microcontroller and stores the upper eight bits in a "shadow register" (the high byte register) at this time. The second part of the read operation pulls data from the high byte register and sends it to the connected microcontroller, where it is appended with the first byte to reconstruct the full 16-bit value [30].

The raw data measurements taken from the color sensor reveal the amounts of red, green, and blue light that compose the unfiltered light. These measurements are then taken and used to calculate the color temperature of the light in degrees Kelvin and the lux in lumens per square meter. The first step to finding these two values was to convert the raw color values (red, green, and blue) from the RGB color space to the CIE 1931 XYZ color space (XYZ) [42, 43]. This was done through applying the formulae in Figure 11 with values that Adafruit derived for use in their sample Arduino code [41]. The second step was to use the resulting values to calculate the "x" and "y" normalized chromaticity coordinates by applying the formulae in Figure 12. The third step was to calculate the inverse line slope "n" from the calculated chromaticity coordinates (also shown in Figure 12). McCamy's formula [44], shown in Figure 13, was used in the next step to calculate the correlated color temperature (CCT) of the measured light value from the sensor. The final step was to use the original raw values in the formula provided by Adafruit (also shown in Figure 13) to calculate the lux of the light hitting the color sensor [41].

$$X = (-0.14282 * redValue) + (1.54924 * greenValue) + (-0.95641 * blueValue)$$
$$Y = (-0.3266 * redValue) + (1.57837 * greenValue) + (-0.73191 * blueValue)$$
$$Z = (-0.68202 * redValue) + (0.77073 * greenValue) + (0.56332 * blueValue)$$

Figure 11: Equations used to convert the measured raw color values from the RGB color space to the XYZ color space.

$$xc = \frac{X}{(X+Y+Z)} \qquad yc = \frac{Y}{(X+Y+Z)} \qquad n = \frac{(xc - 0.3320)}{(yc - 0.1858)}$$

Figure 12: Equations used to calculate the "x" and "y" normalized chromaticity coordinates and inverse slope using the results from the equations in Figure 11.

$$color\ temperature = (449.0 * n^3) + (3525.0 * n^2) + (6823.3 * n) + 5520.33$$
$$lux = (-0.32466 * redValue) + (1.57837 * greenValue) + (-0.73191 * blueValue)$$

Figure 13: Equations used to calculate the color temperature and lux of the incident light on the color sensor from the results of the equations shown in Figure 12.

5.2 Data Processing: Artificial Light

5.2.1 Control Tests

To reliably identify different types of light using the TCS34725, we established a baseline of control data by measuring the light output from different types of light bulbs for periods of 15-20 minutes each. While this means that some of the control tests have a few more data points than others, we determined while testing the initial setup before starting the data collection that this would have a negligible effect on the data collected from artificial light. Nine light bulbs were measured: three incandescent, three fluorescent, and three LED. The characteristics of each light bulb as described on their packaging can be seen in Table 1. The bulbs are organized through a code consisting of the first three letters of "Incandescent", "Fluorescent", or "LED", followed by a number representing the order that the specific type of bulb was tested in.

Bulb Code	Power Consumption	Specified Brightness (lumens)	Package Description
Inc1	29W (40W replacement)	430	"Crystal Clear"
Inc2	25W	210	"Soft White"
Inc3	25W	215	"Crystal Clear"
Flu1	13W (60W replacement)	800	"Natural Daylight (5000K)"
Flu2	13W (60W replacement)	900	"Cool White (4100K)"
Flu3	13W (60W replacement)	850	"Soft White (2700K)"
LED1	2W	180	Unspecified
LED2	5W	250	"Warm Candle Light"
LED3	4W (40W replacement)	300	"Daylight"

Table 1: List of all light bulbs (artificial light sources) used in the characteristic-identification control tests for artificial light

We ran the control tests with the different light bulbs in a closed testing environment that contained an LPCSB and a lamp providing the sole illumination. The lamp used in the tests was a “Decorative Spot Light (Bronze Finish)” manufactured by the company “Portfolio”. Two tests were run for each light bulb; the lamp was placed around 10cm away from the lamp for the first test (a short-range test) and 22 cm away for the second test (a long-range test). Different distances were tested to examine how the LPCSB’s distance away from the light would affect the measurements because measured light intensity decreases as distance from a point source increases [45]. An uncovered example short-range test setup and the control environment enclosure can be seen in Figure 14.

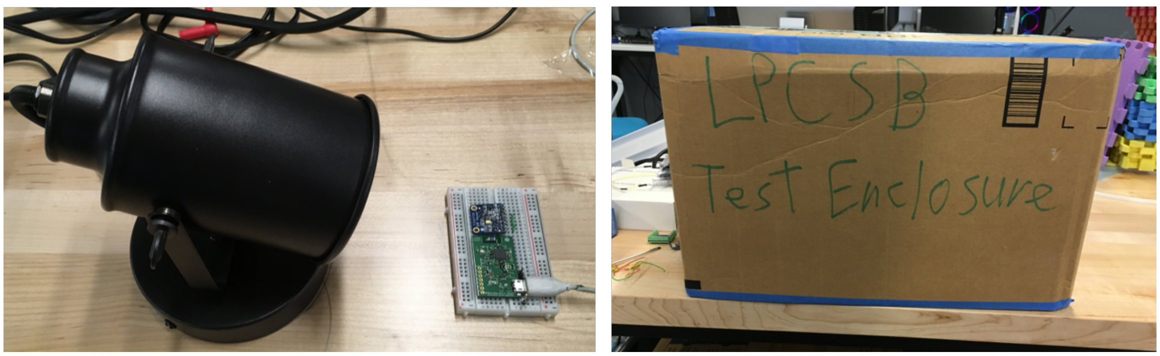

Figure 14: An example short-range test setup and the control environment enclosure

For every control test run, we turned the lamp on first, after which we sealed off the test environment from all external light before activating the LPCSB. When activated, the LPCSB takes about five seconds to configure the nRF51822 and the TCS34725 before making its first measurement. After the LPCSB completed a measurement, it would advertise a BLE data packet containing the hex ID value of the sensor, the raw data (clear, red, green, and blue) split into two bytes per color, the calculated color temperature and lux of the measured light (also split into two bytes per color) and the number of the packet being broadcast. Whenever an LPCSB is activated, its packet number is reset to zero and incremented every time that a packet is advertised.

In the original control tests, the LPCSB did not execute any onboard processing or analysis of the raw data from the TCS34725 nor identify the type of light that the sensor measured. These functionalities were offloaded to a desktop computer that detected the broadcasts from the LPCSB using a Bluegiga BLED112 Bluetooth Smart Module designed to measure any BLE data transmission in its vicinity. Running on the desktop computer was a Python script based off of the “bglib” Github repository [46]. The original script used the BLED112 to detect any BLE advertisement that it could and display the information inside the packet in a command line terminal. For the control tests in this research, we modified the original script in two ways. First, we changed the script so it would only display the data transmitted from a device with a specific MAC address. In this case, it was the LPCSB with the address C0:98:E5:40:60:6C. Along with the raw data broadcast from the LPCSB, the script extracted the name of the device that made the transmission, the device's MAC address, the timestamp (date and time shown on the desktop computer) when the data packet was received, and the Received Signal Strength Indicator (RSSI) of the transmission. We also modified the script to extract the raw color data and the calculated color temperature and lux, calculate the ratios of the maximum color value to the middle color value, the middle color value to the minimum color value, and a new ratio formed by dividing the just-mentioned first ratio by the second, as well as to save each reading to a Microsoft Excel spreadsheet. The readings from the different light bulbs were compared to find the differences between them for use in identifying the type of light bulb being measured. Figure 15 shows a block diagram setup describing how the data-saving algorithm works in conjunction with the LPCSB.

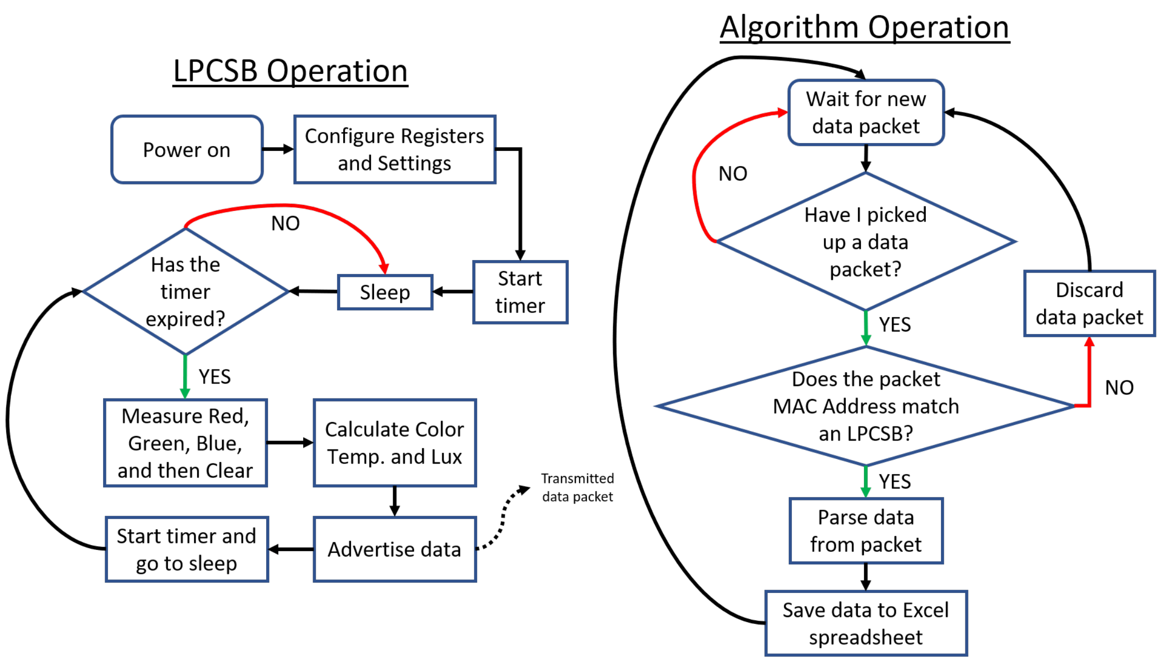

Figure 15: Block diagram showing how the LPCSB and the data-processing algorithm operate in parallel.

5.2.2 Artificial Light Identification Characteristics

Basic observation of graphed raw RGB color data sampled by the LPCSB shows that there are very noticeable differences between the light emitted from different types of light bulb. With three different light bulbs in each category of light, data for incandescent light was the most consistent between bulbs. For each incandescent bulb tested, the raw red color values were the highest of the measured color values. The raw green and blue color values were close enough that the ratio of the larger to the smaller of the two values was less than 1.1. Figure 16 shows the graphed raw color data for each incandescent bulb in both short and long-range tests.

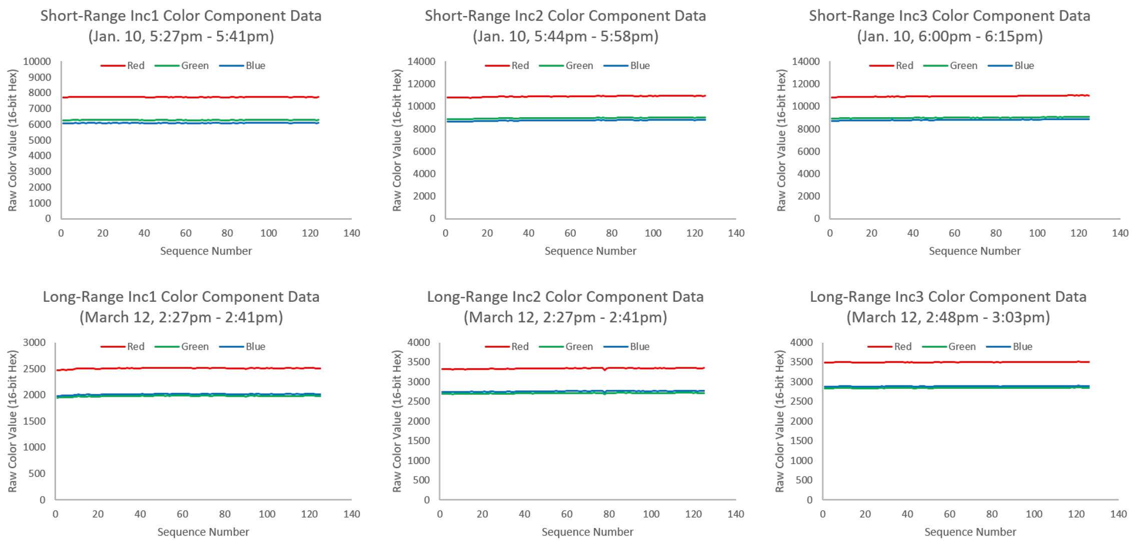

Figure 16: Short and long-range color component control data measured from the incandescent light bulbs. The line colors correspond to specific filters in the TCS34725 photodiode array

The data measured from the three tested fluorescent bulbs was visibly different from the incandescent bulbs. Unlike the incandescent bulbs, the fluorescent bulbs showed green as their highest color value for all control tests, except for the third long-range test. In addition, the majority of raw color values from the tested fluorescent bulbs were lower than those of the incandescent bulbs. The raw color values for the fluorescent bulbs varied the most over time out of the different types of light bulb tested. Figure 17 shows the graphed raw color data for each fluorescent bulb in both short and long-range tests.

Similar to the incandescent bulbs, the LED bulbs showed red as their highest color value for all control tests, except for the third short-range test. The ratios of the maximum to the middle colors and the middle to the minimum colors varied too much in between bulbs to be a reliable identifying characteristic. Also like the incandescent bulbs, the LED bulbs had very steady raw color values, with very little change to the numbers over time. However, the color values were also universally lower than the incandescent values. Figure 18 shows the graphed raw color data for each LED bulb in both short and long-range tests.

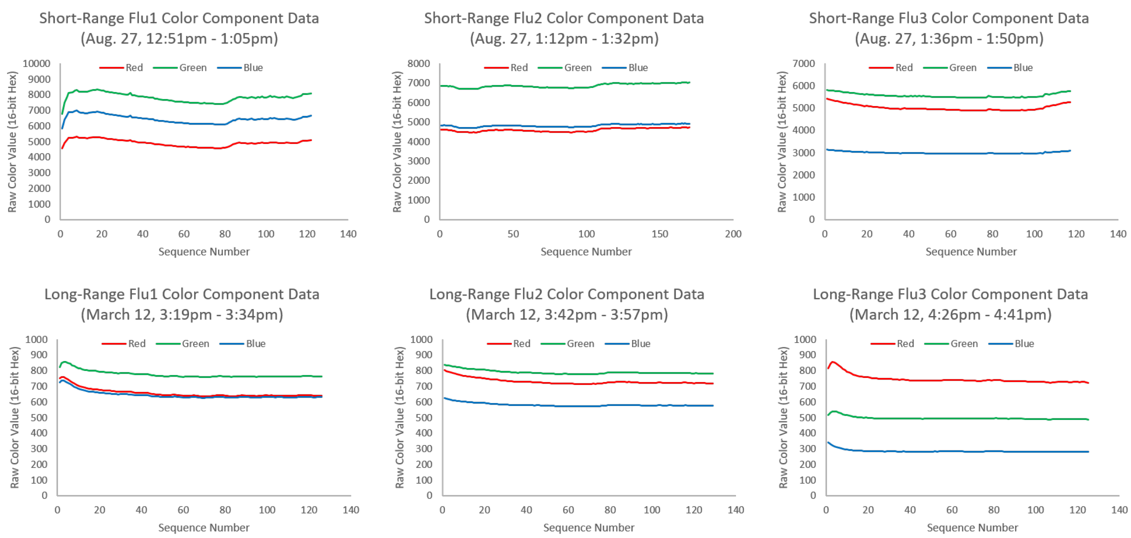

Figure 17: Short and long-range color component control data measured from the fluorescent light bulbs. The line colors correspond to specific filters in the TCS34725 photodiode array.

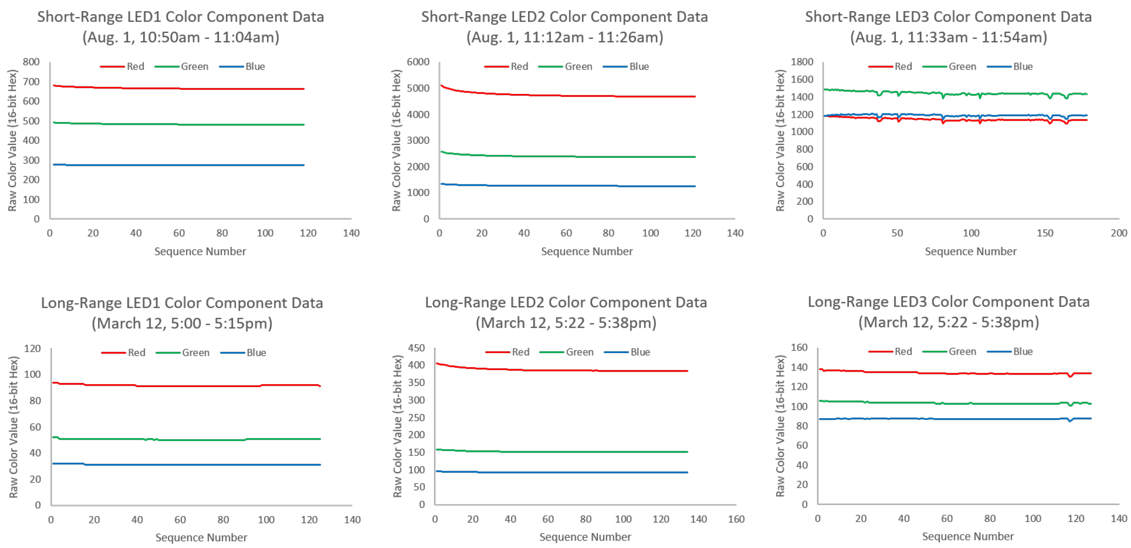

Figure 18: Short and long-range color component control data measured from the LED light bulbs. The line colors correspond to specific filters in the TCS34725 photodiode array.

5.3 Data Processing: Natural Light

5.3.1 Control Tests

The control tests involving natural daylight could not be conducted with the test environment used for the artificial light control tests. For the sunlight tests, the LPCSB used for the artificial light control tests was placed on a window sill in a laboratory such that ambient outdoor light (not direct sunlight) fell on the LPCSB. All lights in the lab were turned off and incoming light from elsewhere in the building was blocked by an opaque cover placed behind the LPCSB to prevent any interference with the daylight measurements. The data was broadcast to the desktop computer from the LPCSB and saved to a Microsoft Excel spreadsheet in the same manner as in the control tests measuring artificial light.

5.3.2 Identification Characteristics

Unlike the artificial light sources, the natural daylight measurements changed a lot more over time. We ran the initial sunlight control tests (Sun1, Sun2, and Sun3) for the same amount of time as the artificial light control tests (15-20 minutes), but it was very hard to identify any common characteristics from the measured data from those tests. When initial tests were run to try identifying sunlight from the observed characteristics, the LPCSB could not recognize sunlight; instead it identified the sunlight as fluorescent light. After further observation, we discovered that this was due to how sunlight fluctuates over time and that the characteristics for sunlight specified in the identification algorithm were very similar to those used for fluorescent light. As a result, we decided to run more control tests in the same location as the original, but over six-hour periods to get a more complete picture of how sunlight changes over time. These tests were identified as “Sun4” through “Sun7”. Table 2 describes the outdoor weather conditions for each of the sunlight tests.

Light Code	Weather Conditions
Sun1	Mostly sunny
Sun2	Mostly cloudy / overcast
Sun3	Mostly sunny
Sun4	Sunny / clear, few to no clouds
Sun5	Partly sunny / slightly overcast – stratus clouds across the sky during the day
Sun6	Cloudy / overcast / rainy
Sun7	Cloudy for the first part, sunny for the rest. See Figure 18 for more details.

Table 2: List of different lighting conditions used in the characteristic-identification control tests for natural light

Analysis of the new data revealed more comprehensive identifying characteristics in each dataset that were missed because the original sunlight measurements were taken over a shorter time period. For all tests, no matter the weather conditions outside, the highest raw color values were either blue or red. When it was sunny and clear outside with very few or no clouds, the measured data changed very smoothly, increasing steadily during the morning until around 12-1pm, and then decreasing as the day progressed. When there were more clouds or the weather was overcast / rainy, there was a lot more fluctuation in the measured values, although they still followed the overall trend of increasing until 12-1pm and then decreasing as the day continued. Figure 19 shows the graphed color data for “Sun1” through “Sun3”, and Figure 20 shows the data for “Sun4” through “Sun7”.

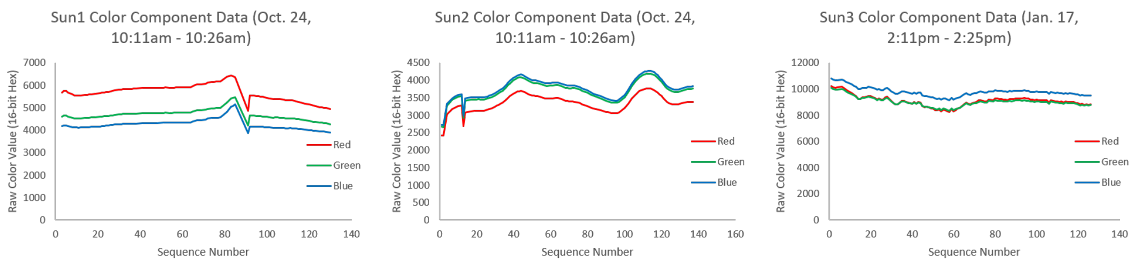

Figure 19: Color component control data measured from Sunlight over a 15-16-minute time period. The line colors correspond to specific filters in the TCS34725 photodiode array.

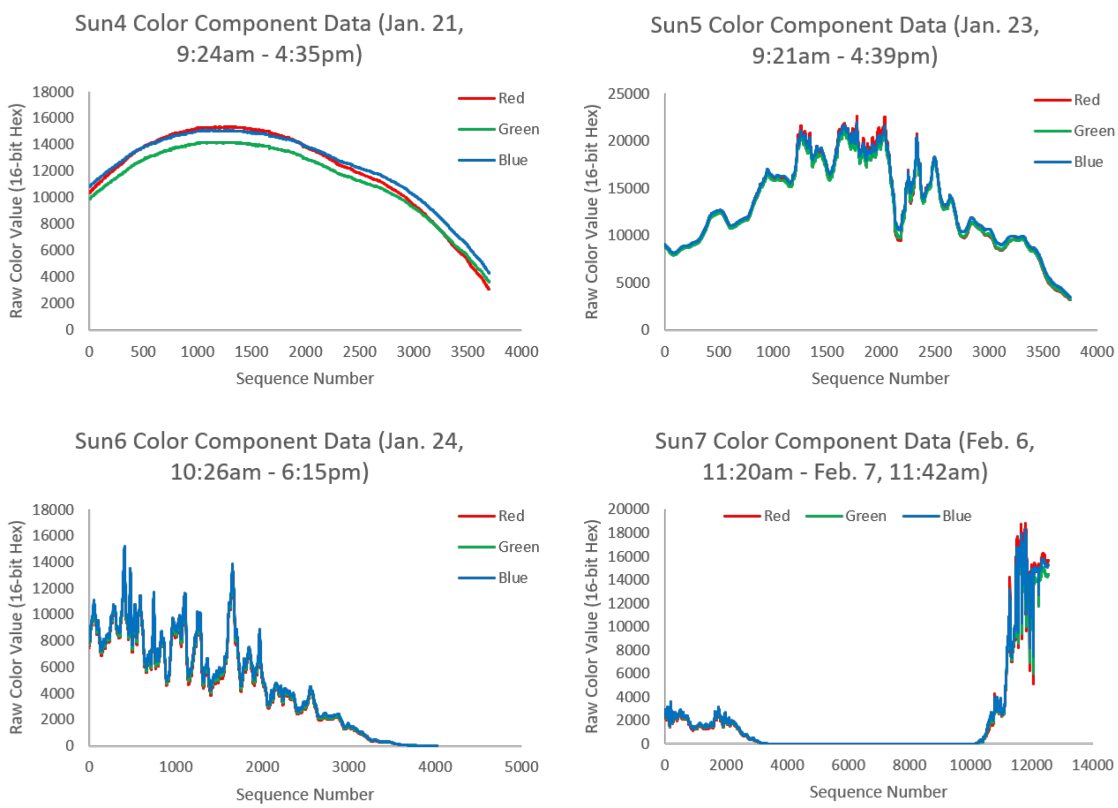

Figure 20: Color component control data measured from Sunlight for longer time periods. The line colors correspond to specific filters in the TCS34725 photodiode array (e.g. the red line with the red-filtered photodiodes). Sun4-Sun6 were measured over a 6-8-hour time period. Sun7 was measured over a 24-hour time period. The first part of Sun7 (Feb. 6 measurements) was cloudy, while the second part (Feb. 7) was sunnier. The sequence number range in Sun7 from 3,274-10,228 corresponds to between 5:42pm on Feb. 6 and 7:13am on Feb. 7 (nighttime).

Chapter 6

Evaluation

6.1 Identification Algorithm

6.1.1 Development

After the original control tests were completed, we made a copy of data-saving script that was modified to use the characteristics derived from the control tests to identify the type of light shining on the LPCSB before saving the data to a specified Excel spreadsheet. The algorithm was developed through an iterative design process and was based around the identifying characteristics of each type of light that were distinguished through visual analysis of the data obtained from the control tests. We designed the algorithm as a series of if-statements that would check if the currently measured data point met specific requirements, and to have the algorithm identify different types of light based on these requirements. The requirements were derived from the identified characteristics of each type of measured light in the control tests, and the requirements were checked in an order that was based on how easy it was to identify the distinguishing characteristics of the different types of light.

6.1.2 Incandescent Characteristics

First, the characteristics of incandescent light as described earlier were the easiest to identify. No other type of light bulb from the ones shown in Table 1 had the exact same set of characteristics as the incandescent ones; therefore, the distinguishing characteristics of incandescent light described when discussing the artificial light control test results were checked first. The specific conditions in the if-statement for incandescent light were that the maximum raw color value measured from the

TCS34725 was red, that the ratio of the maximum color value (red) to the middle color value was greater than 1.15, and that both the middle and minimum raw color values (green and blue or vice versa) were close enough to each other that the ratio of the middle value to the minimum value was less than 1.05. These threshold values were obtained through trial and error, starting with the values obtained in the collected data and adjusting them so there would be a small buffer between the measured values and the threshold values that would hopefully account for incandescent light bulbs not measured in the control tests.

6.1.3 Fluorescent Characteristics

The next set of characteristics for the algorithm to check were the ones for fluorescent light. They were more difficult than incandescent light, because while green was the highest raw color value for the majority of the fluorescent control tests, one of the measured light bulbs had red as the highest raw color value in its test. This was dealt with by having the algorithm check if the maximum value was green, or if the maximum value was red, green was the second-highest value, and green was close to red (the ratio of green to red was less than or equal to 1.1).

6.1.4 LED Characteristics

LEDs were the third type of light checked. As stated earlier, LED was similar to incandescent because the majority of highest raw color values were also red. However, we could not check for red as the highest color again because one of the LED bulbs had green as its highest raw color value. After some thought, we noticed that the measured incandescent and LED raw color values both changed very little over time. We decided to have the algorithm check the magnitude of the value change over time, with the measured light being classified as LED if the absolute value of the change was less than or equal to a threshold value. The change was calculated by taking the difference between the newest measured color values and the immediately preceding ones and adding it to a total. After testing a lot of different net values, we settled on using 200 as our threshold.

6.1.5 Sunlight Characteristics

Sunlight varied the most over time and it was difficult to find consistent identifying characteristics for it, so it was set as the last type of light to check for. For checking distinguishing characteristics, we settled on a similar approach to fluorescent, checking to see if blue was the highest value or if blue was the second-highest value but close enough to the highest that the ratio of the highest to second-highest value was 1.05. Any data points that did not meet the requirements for sunlight were classified as “Unknown”.

6.1.6 Algorithm Adjustments

The completed algorithm was able to identify artificial light in preliminary testing using the conditions described above. However, when tested with sunlight, the algorithm would always identify the measured light as fluorescent light. After further analysis, we noticed that the magnitude of sunlight values was almost always higher than all of the artificial light measurements, so we went back and modified the algorithm to add thresholds for the magnitude of the raw color value for some of the types of light. After testing a variety of options, we settled on values greater than or equal to 2,000 and less than 10,000 for fluorescent light, and less than or equal to 2,000 for LED light. We left the incandescent requirements alone because none of the other tested light bulbs had the same color profile as the incandescent ones. After adding the threshold values to the algorithm, the algorithm was able to differentiate between fluorescent light and sunlight. Figure 21 shows how the original algorithm was modified to classify the measured light, as well as pseudocode of the algorithm itself, and also includes some minor changes that were made for reasons described later. We ran the light-identification tests with the same setup and duration as in the characteristic-identification tests, with the same light bulbs used in the characteristic-identification tests (Table 1).

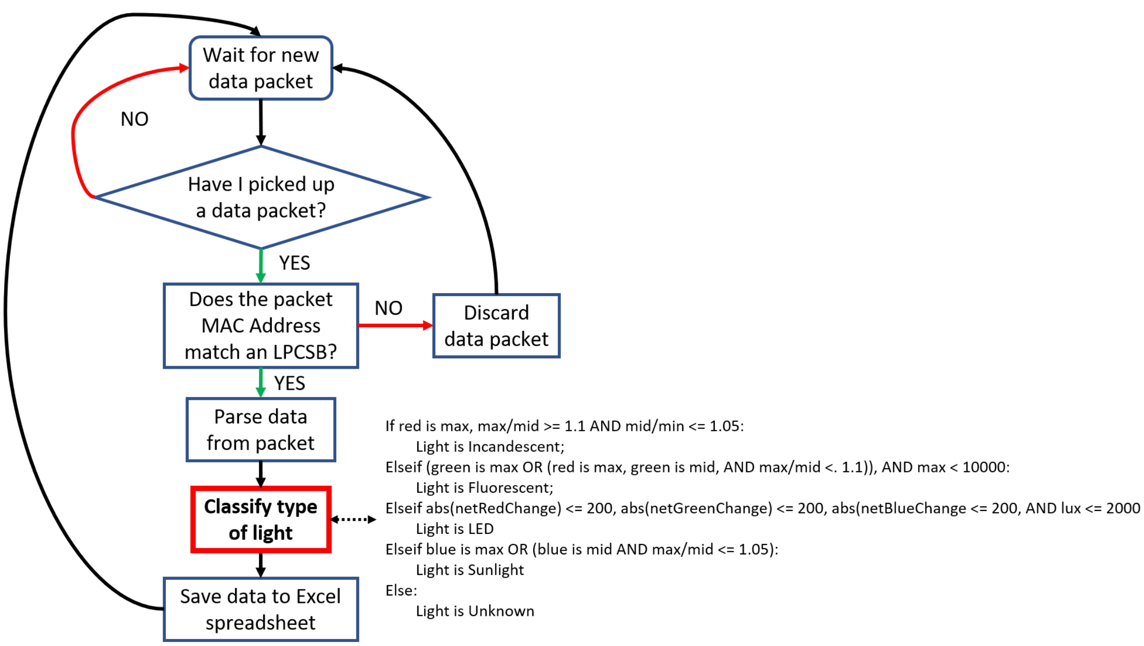

Figure 21: Block diagram of the data-processing algorithm modified to classify the measured light before saving to Excel, and pseudocode of the conditions that are examined for each type of light.

6.2 Identification Tests: Artificial Light

Incandescent

Initially, we did not consider the distance of the LPCSB from the light source in the control environment when identifying the characteristics of artificial light, which led to dismal results from the algorithm when the LPCSB was tested at 22 cm away from the light source instead of 10 cm. Once we realized that the distance from the light source was important, we adjusted the identification algorithm to take this into account and become more robust to variations in the ambient light. When tested, the revised algorithm successfully recognized all three incandescent light bulbs 100 % of the time in both short and long-range tests, as shown in Figure 22.

Light Type	Description	Inc1 Short	Inc2 Short	Inc3 Short
Incandescent	Number of times "Incandescent" appears	480	342	220
Fluorescent	Number of times "Fluorescent" appears	0	0	0
LED	Number of times "LED" appears	0	0	0
Sunlight	Number of times "Sunlight" appears	0	0	0
Unknown	Number of times "Unknown" appears	0	0	0

Light Type	Description	Inc1 Long	Inc2 Long	Inc3 Long
Incandescent	Number of times "Incandescent" appears	170	217	284
Fluorescent	Number of times "Fluorescent" appears	0	0	0
LED	Number of times "LED" appears	0	0	0
Sunlight	Number of times "Sunlight" appears	0	0	0
Unknown	Number of times "Unknown" appears	0	0	0

Light Type	Description	Inc1 Total	Inc2 Total	Inc3 Total
Incandescent	Number of times "Incandescent" appears	650	559	504
Fluorescent	Number of times "Fluorescent" appears	0	0	0
LED	Number of times "LED" appears	0	0	0
Sunlight	Number of times "Sunlight" appears	0	0	0
Unknown	Number of times "Unknown" appears	0	0	0

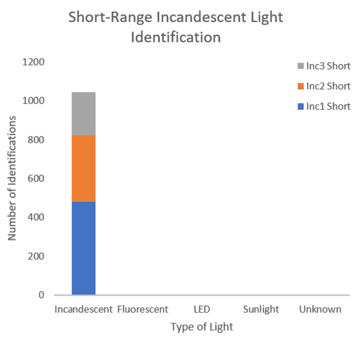

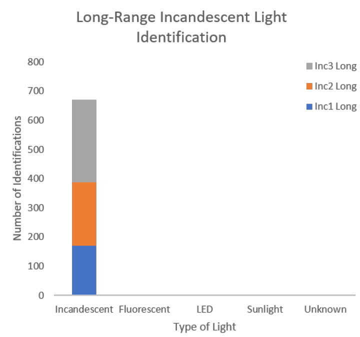

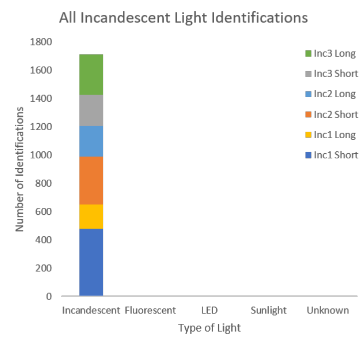

Figure 22: Identification of incandescent light bulbs in both short and long-range tests.

Fluorescent and LED

The revised algorithm was less successful with fluorescent light bulbs. While it successfully recognized all three of the bulbs in the short-range tests, it consistently identified one of the bulbs as LED in the long-range tests. The algorithm performed similarly with LED bulbs; it recognized one of the LED bulbs as fluorescent in the short-range tests but successfully identified all of the LED bulbs in the long-range tests. Figures 23 and 24 display the performance of the identification algorithm with fluorescent and LED bulbs in short and long-range tests respectively.

Real-World: Ceiling LED

After running identification tests on the light bulbs used in the control tests, we tested the LPCSB and the identification algorithm in the normal environment of the Link Lab in the early evening

Light Type	Description	Flu1 Short	Flu2 Short	Flu3 Short
Incandescent	Number of times "Incandescent" appears	0	0	0
Fluorescent	Number of times "Fluorescent" appears	277	127	168
LED	Number of times "LED" appears	0	0	0
Sunlight	Number of times "Sunlight" appears	0	0	0
Unknown	Number of times "Unknown" appears	0	0	0

Light Type	Description	Flu1 Long	Flu2 Long	Flu3 Long
Incandescent	Number of times "Incandescent" appears	0	0	0
Fluorescent	Number of times "Fluorescent" appears	256	250	0
LED	Number of times "LED" appears	0	0	226
Sunlight	Number of times "Sunlight" appears	0	0	0
Unknown	Number of times "Unknown" appears	0	0	0

Light Type	Description	Inc1 Total	Inc2 Total	Inc3 Total
Incandescent	Number of times "Incandescent" appears	0	0	0
Fluorescent	Number of times "Fluorescent" appears	533	377	168
LED	Number of times "LED" appears	0	0	226
Sunlight	Number of times "Sunlight" appears	0	0	0
Unknown	Number of times "Unknown" appears	0	0	0

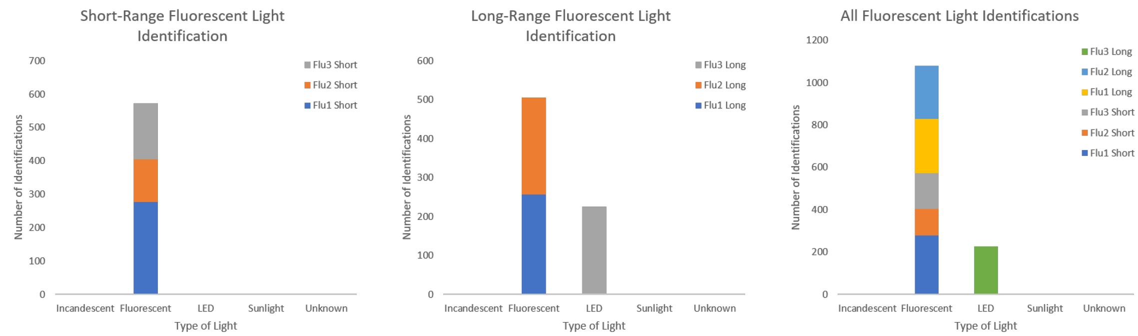

Figure 23: Identification of fluorescent light bulbs in both short and long-range tests.

Light Type	Description	LED1 Short	LED2 Short	LED3 Short
Incandescent	Number of times "Incandescent" appears	0	0	0
Fluorescent	Number of times "Fluorescent" appears	0	0	292
LED	Number of times "LED" appears	272	257	0
Sunlight	Number of times "Sunlight" appears	0	0	0
Unknown	Number of times "Unknown" appears	0	0	0

Light Type	Description	LED1 Long	LED2 Long	LED3 Long
Incandescent	Number of times "Incandescent" appears	0	0	0
Fluorescent	Number of times "Fluorescent" appears	0	0	0
LED	Number of times "LED" appears	247	264	263
Sunlight	Number of times "Sunlight" appears	0	0	0
Unknown	Number of times "Unknown" appears	0	0	0

Light Type	Description	LED1 Total	LED2 Total	LED3 Total
Incandescent	Number of times "Incandescent" appears	0	0	0
Fluorescent	Number of times "Fluorescent" appears	0	0	292
LED	Number of times "LED" appears	519	521	263
Sunlight	Number of times "Sunlight" appears	0	0	0
Unknown	Number of times "Unknown" appears	0	0	0

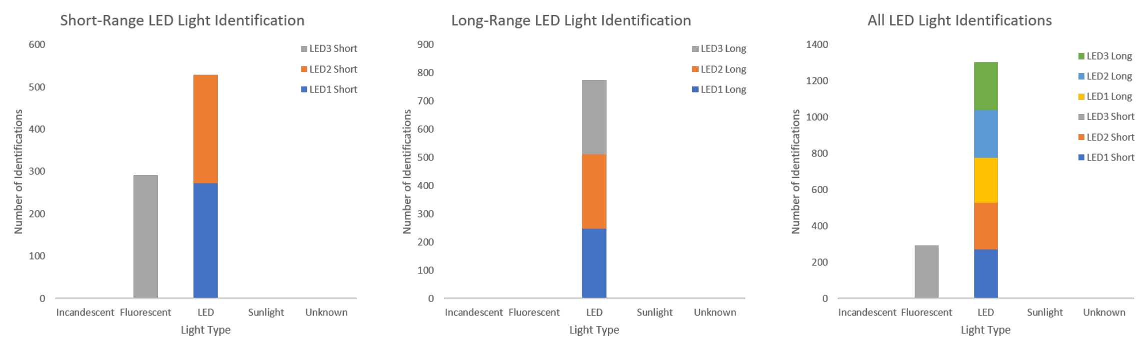

Figure 24: Identification of LED light bulbs in both short and long-range tests.

to see if the type of light normally illuminating the lab (LED ceiling lights) could be identified. This test was run in the afternoon with all windows covered by blinds to see if the LPCSB could reliably identify light from a source that was not tested during the characteristic-identification tests. The LPCSB was positioned on the same table in the middle of the room that was used in the characteristic identification tests, secured in place, and left uncovered. The algorithm was able to identify the ceiling lights as LED 100 % of the time, as shown in Figure 25.

It should be noted that while running the identification tests with the light bulbs used in the control tests, we placed only one lightbulb in the closed environment at a time. Since the intensity of light on a surface is related to distance through an inverse square relationship [45], the intensity of light landing on the TCS34725 decreases proportionally as it is moved further away from the sensor. However, in real-world environments like the UVA Link Lab, there is usually more than one light

Light Type	Description	Output
Incandescent	Number of times "Incandescent" appears	0
Fluorescent	Number of times "Fluorescent" appears	0
LED	Number of times "LED" appears	320
Sunlight	Number of times "Sunlight" appears	0
Unknown	Number of times "Unknown" appears	0

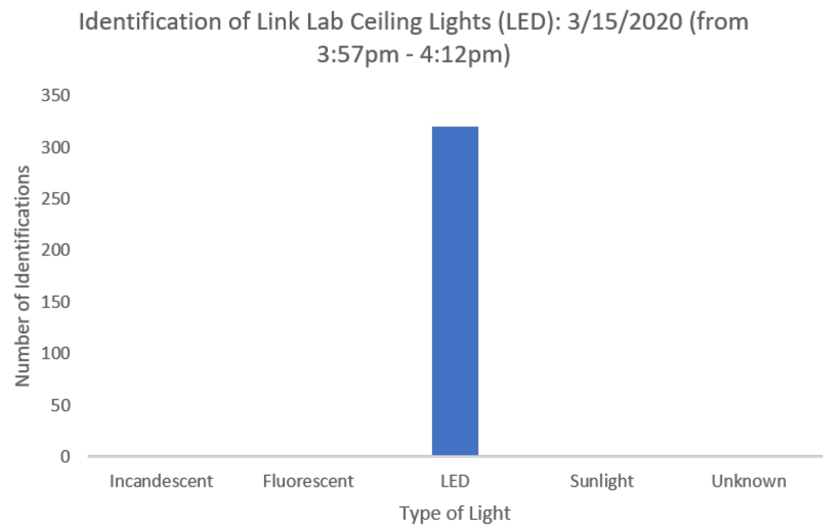

Figure 25: Identification of the Link Lab LED ceiling lights.

bulb or source of light used to illuminate a large area, and these sources of light are not concentrated in a single location.

6.3 Identification Tests: Natural Light

After testing the identification algorithm with the bulbs used in the control tests and the Link Lab ceiling lights, four tests to identify sunlight were run under different weather conditions. We ran the tests over a period of six to eight hours, in the same timeframe as some of the sunlight control tests (Sun4, Sun5, and Sun6) were run for. The performance of the algorithm varied depending on the outdoor weather conditions.

First Test

For the first identification test of sunlight, run on February 5, 2020, the weather was mostly cloudy / overcast, with intermittent light rain / drizzle throughout the day. Under these conditions, the LPCSB made 3611 data measurements. With the received data packets, the algorithm could correctly identify sunlight only 35.1 % of the time. Figure 26 shows the performance of the identification algorithm under the described weather conditions.

Light Type	Description	Output
Incandescent	Number of times "Incandescent" appears	0
Fluorescent	Number of times "Fluorescent" appears	541
LED	Number of times "LED" appears	1184
Sunlight	Number of times "Sunlight" appears	933
Unknown	Number of times "Unknown" appears	0

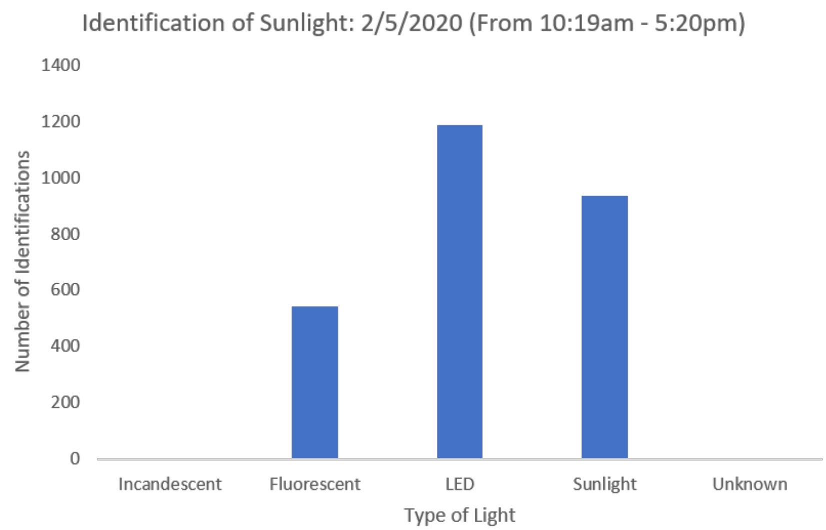

Figure 26: Identification of sunlight in cloudy / overcast weather with intermittent / light drizzle throughout the day.

Second Test

The conditions for the second sunlight identification test (run on February 7, 2020) were markedly different from the first; the skies were partly cloudy / fair throughout the day. Under these conditions, 3129 data measurements were made. With the received data packets, the algorithm correctly identified sunlight 87.42 % of the time, a very noticeable improvement over its performance in the previous test. Figure 27 shows the performance of the algorithm under these conditions.

Third Test

We ran the third sunlight identification test on February 24, 2020. The weather conditions on this day were similar those in the first test. However, while the skies were mostly cloudy / overcast as on the first day, there was no rainfall and the light was brighter. Under these conditions, the identification

Light Type	Description	Output
Incandescent	Number of times "Incandescent" appears	0
Fluorescent	Number of times "Fluorescent" appears	0
LED	Number of times "LED" appears	0
Sunlight	Number of times "Sunlight appears	2731
Unknown	Number of times "Unknown" appears	393

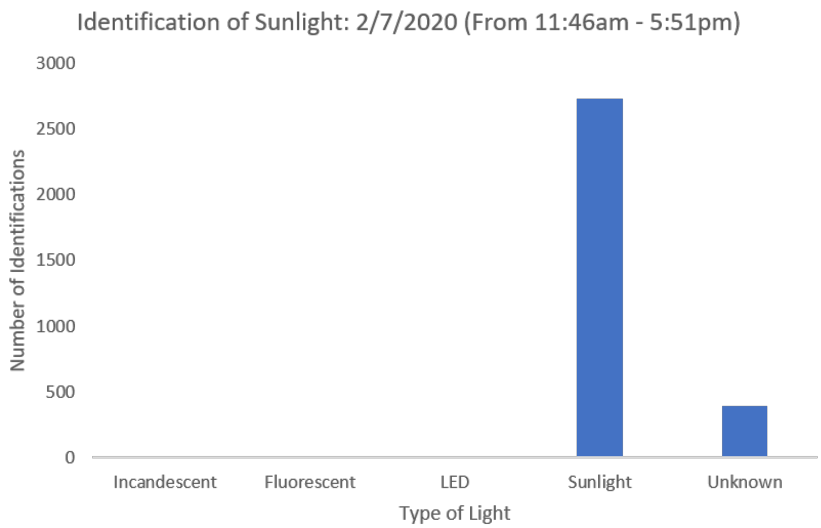

Figure 27: Identification of sunlight in partly cloudy / fair weather, intermittent sunshine.

algorithm correctly identified sunlight 100 % of the time. Figure 28 shows the performance of the algorithm under these weather conditions.

Fourth Test

A fourth sunlight identification test was run on February 27, 2020. The weather conditions on this day were sunny, with very few to no clouds for the majority of the day. Under these conditions, the identification algorithm was correct 74.74 % of the time. Of the remaining identifications, the majority were fluorescent, with only eight points identified as "Unknown". However, this test was run longer than the other three identification tests, ending at around 8:15pm. The other three tests ended between 5:00pm and 6:00pm on the day of each respective test. In this test, there is a clear cutoff line between when the LPCSB stopped identifying sunlight and started identifying fluorescent light, with the first fluorescent identification occurring at 6:22pm. Sunset on February 27 was at 6:05pm in Charlottesville Virginia. If all of the data from the fourth identification test after sunset (6:05pm) is excluded to focus only on measurements made during the daytime, then the identification algorithm becomes 99.81 % correct. All of the "Unknown" measurements were made during the time period that the sun was above the horizon. Figure 29 shows the performance of the

Light Type	Description	Output
Incandescent	Number of times "Incandescent" appears	0
Fluorescent	Number of times "Fluorescent" appears	0
LED	Number of times "LED" appears	0
Sunlight	Number of times "Sunlight appears	4489
Unknown	Number of times "Unknown" appears	0

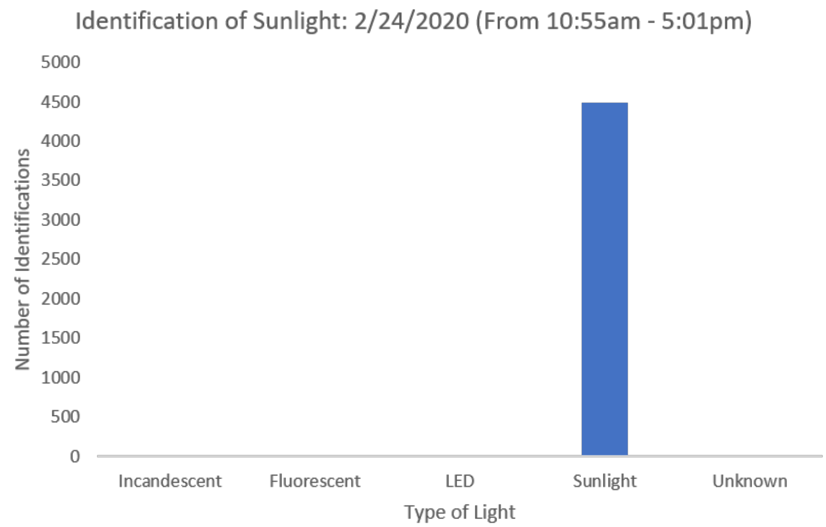

Figure 28: Identification of sunlight in cloudy / overcast weather, no rain. Ambient light was brighter than during the first sunlight identification test.

identification algorithm with all data points, as well as the performance of the algorithm with just the data points that were measured before sunset.

6.4 Aggregation of Results

Overall, the identification algorithm was very effective at identifying both sunlight and different types of artificial light. As described above, however, there were a number of misclassifications in the identification tests of both natural and artificial light. Figure 30 shows confusion matrices that display how many correct and incorrect identifications were made for each type of light in short-range tests with artificial light, long-range tests with artificial light, and both short and long-range tests together with sunlight. The matrices were generated in MATLAB. To generate the matrices, we combined the classifications from each identification test in a specific light category together into one big matrix and compared the matrix with a new one-column matrix of the same size containing a value of the known light category in each index. For example, all of the classifications in the sunlight identification tests were organized into a one-column matrix and then compared with a matrix that

Light Type	Description	Output
Incandescent	Number of times "Incandescent" appears	0
Fluorescent	Number of times "Fluorescent" appears	1438
LED	Number of times "LED" appears	0
Sunlight	Number of times "Sunlight appears	4279
Unknown	Number of times "Unknown" appears	8

Light Type	Description	Output
Incandescent	Number of times "Incandescent" appears	0
Fluorescent	Number of times "Fluorescent" appears	0
LED	Number of times "LED" appears	0
Sunlight	Number of times "Sunlight appears	4134
Unknown	Number of times "Unknown" appears	8

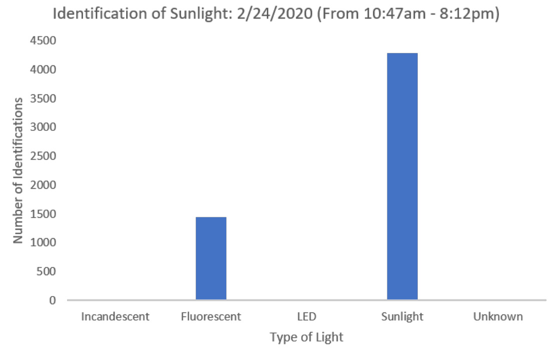

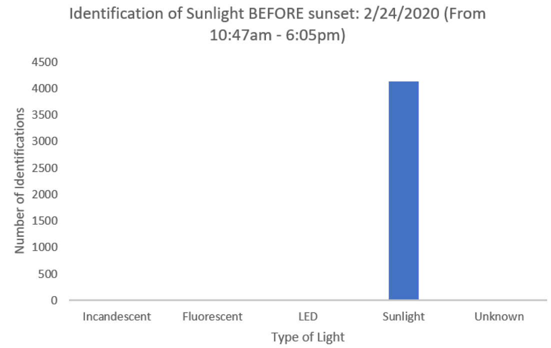

Figure 29: Identification of sunlight in sunny weather, with few-no clouds. Sunset on this day (2/24/2020) was at around 6:22pm.

contained "Sunlight" in each index. This was repeated for each type of light, after which the script used all of the results to generate the matrices.

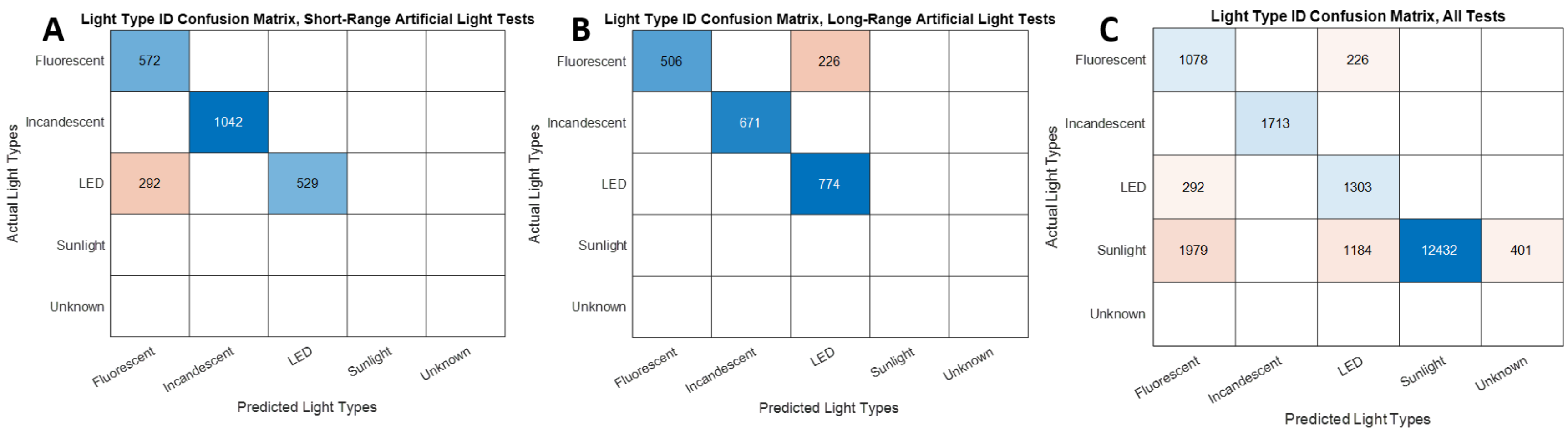

Figure 30: Confusion matrices displaying the number of correct and incorrect classifications for both short-range and long-range artificial light identification tests (A. and B., respectively), and both together with sunlight (C.). Numbers of correct classifications are shown in shades of blue and numbers of incorrect classifications are shown in shades of red. The blue and red shades are rendered in deeper hues as the number of classifications in corresponding sections of the matrix increases. For example, 292 measurements in A. that should have been classified as LED were misclassified as Fluorescent and 226 measurements in B. that should have been classified as Fluorescent were misclassified as LED.

Chapter 7

Limitations and Future Work

7.1 Light Bulbs Tested

While the results from the initial light-type identification tests run with the LPCSB appear promising, they should be interpreted with caution and several limitations need to be considered. In the original control tests, we tested only three light bulbs for each type of artificial light (nine bulbs total), which could limit the efficacy of the light identification algorithm if other bulbs have different identifying characteristics from the ones tested. When running the control tests, we did not test light bulbs with colored glass in detail. Only one of the control bulbs (LED2) had colored glass (amber), which is not enough of a sample size to say whether colored glass affects the characteristics of the measured light to a noticeable degree. Furthermore, when the data was being analyzed, we observed the identifying characteristics for each type of light by eye. There is room for error in this because the observed characteristics may not necessarily apply to other light bulbs not tested in this work. Further studies should expand the pool of light bulbs tested to create a more complete record of the characteristics of each type of light.

Due to the focus on the ability to identify a single type of light, there was not enough time to run control tests measuring two or more different types of light bulb at once. Tests with two or more bulbs would have been useful to see if the LPCSB recognized either one or both of the light types, to see if one type of light dominated the control environment over the other, or if the LPCSB would be unable to recognize either of the types of light being measured.

7.2 Test Environments

Inside the control environment, the walls were light brown and the inside of the light bulb socket in the lamp was light brown/red. While it is believed that this did not adversely affect the color of light reaching the LPCSB, future studies should make sure that everything in the environment that is not an illumination source should be a neutral color such as black or white to avoid changing the color of any reflected light that reaches the LPCSB. In addition, the light source for the control tests was placed very close to the LPCSB (around 10 cm and 22 cm for the short-range and long-range tests respectively). Future studies should run additional tests in a larger control environment with the source further away from the LPCSB to gather more observations about how the distance of the light source from the sensor affects the measured data. While we know the relationship between distance and intensity of light, it is still necessary to observe if the identifying characteristics of the measured light change from what was observed at a closer range or if the ratio of the measured colors to each other remains relatively constant. Some of these tests should also include more than one light source of the same type placed in the control environment to better approximate a real-world environment.

Outside the control environment, the types of light illuminating the work environment in the UVA Link Lab were the LED ceiling lights and sunlight from outside. While this was a good environment to test the LPCSB in, it was the only real-world environment besides the control environment that was used for testing artificial light identification. Further studies should see the LPCSB tested in other environments that are illuminated at least in part by incandescent and/or fluorescent light to observe how the results from these environments compare with those of the Link Lab.

7.3 Measurements and Calculations

When measuring sunlight in the identification tests described earlier, the location of the LPCSB was a major factor when examining how to get the most precise data measurements. Another factor that was not considered at the time was the position of the sun itself at the time the measurements were taken. A revised report released in 2008 by the National Renewable Energy Laboratory (NREL) describes "a step by step procedure for implementing an algorithm to calculate the solar zenith and azimuth angles ... with uncertainties of +/- 0.003 degrees" [47]. In future studies, accounting for the location of the sun at the time of the measurement could make the LPCSB identification algorithm much more precise with sunlight than it currently is.

When calculating the color temperature, lux, and color values from the raw sensor measurements, the constants used in McCamy's formula for this specific application were derived by developers in Adafruit Industries as specified in their provided TCS34725 codebase library. The specific method for deriving these values was unclear beyond a statement that the values were derived from "6500 K fluorescent, 3000 K fluorescent, and 60 W incandescent values for a wide range" [41]. Future studies should derive new constants using not just these values, but also values from additional incandescent and LED bulbs, for use in McCamy's formula.

7.4 Power Consumption and Data Processing

7.4.1 Power Consumption

While the LPCSB is meant to consume very little power as a part of the IoT, it currently is not designed to do so. That aspect was not focused on in this work beyond choosing components with low energy consumption; the focus was instead on determining the device's capability to identify artificial and natural light. Currently, the device receives power through a USB cable that plugs either into a computer USB port or a 5 V wall socket plug. A future study with the LPCSB should focus on optimizing it for low power consumption and measuring how this would affect the measurements taken and the identification capability.

7.4.2 Duplicate Packets

Each time that we used the LPCSB for data collection, an estimated 20 % of its data packets were lost in transmission to the desktop computer with the identification algorithm. To combat this, the LPCSB was programmed to transmit each data packet several times to increase the chances that one of them would be received by the computer running the identification algorithm. While it worked, it meant that a number of the received packets from the LPCSB transmissions were duplicates, which may have skewed the percentage of correct and / or incorrect identifications. Further studies should take this into account and figure out a way to reduce the packet loss rate so that duplicate transmissions of the data packets will not be required. A potential option to remove duplicates would be to have the identification algorithm check the received data packets for duplicates based on the packet sequence number and discard / ignore all further data packets until the sequence number changes.

7.5 Onboard and Offload Approaches

7.5.1 Overview

There are also a number of tradeoffs between running the light-classification algorithm on the LPCSB itself (onboard approach) and on an external computer (offload approach). The current iteration of the algorithm operates in the offload approach and classifies each individual measured data point into a category of light.

7.5.2 Onboard Approach

With an onboard approach, there would be no central computer running the light-classification algorithm. If the algorithm is implemented on the LPCSB itself, the LPCSB would need to transmit just one byte of information containing the representation of the category of light that the data point was classified to. This means that the LPCSB would save power when transmitting data, having to send only one byte instead of the several that contain the raw color data from the sensor. The LPCSB would also be more mobile, no longer restricted to a maximum distance away from a central unit running the algorithm. However, this approach would not let us see the raw data from the sensor if the LPCSB classifies the sensor measurement either incorrectly or as "Unknown" before transmitting, unless the LPCSB is programmed to know when this occurs and transmit the raw data. While this could be a potential problem, there is also the possibility that an onboard approach could allow the LPCSB to classify measured light more accurately than the current offload approach.

The nRF51822 processor has enough memory that the LPCSB algorithm could also be modified to take several measurements from the TCS34725 over a period of time and use all of those data points to classify the measured light before transmitting the result. We did develop an early-stage version of the LPCSB software that took the onboard approach such that the LPCSB would be able to identify the type of light from the data point measured and transmit just the classification of the data instead of the raw data itself. However, detailed control and identification tests of sunlight and artificial light with this new setup were not executed due to time constraints. It is also possible that there are more sophisticated algorithms that would work better at classifying light onboard over offload even if they can be implemented successfully in both.

7.5.3 Offload Approach

With the offload approach that this work focuses on, the LPCSB has to transmit a lot of raw data to the computer running the identification algorithm. Because the LPCSB transmits the raw data from the TCS34725 to the computer in this approach, the data packet is larger than it would be if the onboard approach was used. This means that the LPCSB consumes a little more power than it would in the onboard approach because it has to transmit more bytes of data. However, the offload approach does work better for conducting more in-depth analysis of the measured data and for refining the classification algorithm. The offload approach may also be more useful if it is desired to implement a sophisticated machine-learning version of the classification algorithm, allowing for huge datasets to be taken and used to train the algorithm to better classify light. The onboard approach described previously would probably not be a feasible way to do this because of memory constraints on the nRF51822 and the resulting inability to save large amounts of data at once.

7.6 Machine Learning

Last, there is huge potential for implementing machine learning with the LPCSB. There are many other factors that could be incorporated into a machine learning algorithm. The LPCSB could compare data measured directly from the TCS34725 sensor and learn from full saved control test datasets instead of being restricted to merely analyzing each individual data point as it is captured. Data from external environmental factors such as weather conditions could be used to help remove noise and reduce errant measurements when measuring sunlight. Other sensors could be deployed to measure the electricity consumption of the location that an LPCSB is monitoring; the machine learning algorithm could use the data from those measurements in combination with the color data from the TCS34725 to determine if there are any electric lights nearby and whether any artificial light from these sources is overwhelming any sunlight that is reaching the LPCSB. The algorithm could be structured similarly to the one developed by Coley and Crabb (1997), but with access to more data and a wider set of parameters to consider. A fully developed machine learning algorithm would make it much easier to observe how the data from a test changes over time and develop a more complete view of a much more complicated dataset for the algorithm to analyze and get much more precise and accurate results.

Chapter 8

Conclusion

Using an off-the shelf photodiode array, we have demonstrated that different light bulbs have unique characteristics in the visible spectrum of light (red, green, and blue), and these characteristics are consistent across different bulbs in the same category of artificial light. With data measured by said photodiode array, we have developed a new system called the LPCSB that is capable of distinguishing between natural light (sunlight) and different types of artificial light. Initial testing has shown that this setup is very effective at accurately classifying light and doing so consistently. It would be very easy to deploy fully-functioning LPCSB's in a room anywhere near a power source and use it to classify the illuminating light, whether it is being used as a design tool or as part of a larger network of environmental monitoring and connected devices. While there is still much that needs to be done, this new system has the potential to be a very useful tool in the hands of both engineers and architects. We plan to submit the results of this work to the IEEE 6th World Forum on Internet of Things in 2021 (WFIoT2021). This year, the conference (WFIoT2020) was supposed to be held on April 5-9, 2020, in New Orleans, but was postponed due to the COVID-19 pandemic.

References

[1] L. Kellaway, "How the office was invented," *BBC News Magazine*. Accessed: Aug. 30, 2019. [Online]. Available: `https://www.bbc.com/news/magazine-23372401`.

[2] P. Manning, "Office design: A study of environment," 1965.

[3] M. Boubekri, I. N. Cheung, K. J. Reid, C.-H. Wang, and P. C. Zee, "Impact of windows and daylight exposure on overall health and sleep quality of office workers: A case-control pilot study," *Journal of Clinical Sleep Medicine*, vol. 10, no. 06, pp. 603–611, 2014.

[4] M. K. Alimoglu and L. Donmez, "Daylight exposure and the other predictors of burnout among nurses in a university hospital," *International Journal of Nursing Studies*, vol. 42, no. 5, pp. 549–555, 2005.

[5] P. Boyce, C. Hunter, and O. Howlett, "The benefits of daylight through windows," *Troy, New York: Rensselaer Polytechnic Institute*, 2003.

[6] S. Altomonte, "Daylight for energy savings and psycho-physiological well-being in sustainable built environments," *Journal of Sustainable Development*, vol. 1, no. 3, pp. 3–16, 2008.

[7] M. De Carli, V. De Giuli, and R. Zecchin, "Review on visual comfort in office buildings and influence of daylight in productivity," in *11th International Conference Indoor Air, Copenhagen*, 2008.

[8] L. Edwards and P. Torcellini, "Literature review of the effects of natural light on building occupants," tech. rep., National Renewable Energy Lab., Golden, CO.(US), 2002.

[9] T. Chung and J. Burnett, "Lighting quality surveys in office premises," *Indoor and Built Environment*, vol. 9, no. 6, pp. 335–341, 2000.

[10] M. B. Aries, M. P. Aarts, and J. van Hoof, "Daylight and health: A review of the evidence and consequences for the built environment," *Lighting Research & Technology*, vol. 47, no. 1, pp. 6–27, 2015.

[11] M. R. Rosekind, K. B. Gregory, M. M. Mallis, S. L. Brandt, B. Seal, and D. Lerner, "The cost of poor sleep: Workplace productivity loss and associated costs," *Journal of Occupational and Environmental Medicine*, vol. 52, no. 1, pp. 91–98, 2010.

[12] D. Clements-Croome *et al.*, *Creating the productive workplace*. Taylor & Francis, 2006.

[13] Y. S. Lee and S.-K. Kim, "Indoor environmental quality in LEED-certified buildings in the US," *Journal of Asian Architecture and Building Engineering*, vol. 7, no. 2, pp. 293–300, 2008.

[14] T. Holowka, "Indoor environmental quality and LEED v4," *USGBC*. Accessed: Nov. 12, 2019. [Online]. Available: `https://www.usgbc.org/articles/indoor-environmental-quality-and-leed-v4`.

[15] "Leed v4 for building design and construction," *United States Green Building Council Inc*, 2014.

[16] "Ultraviolet Support," *Apogee Instruments*, 2020. Accessed: Dec. 12, 2019. [Online]. Available: https://www.apogeeinstruments.com/ultraviolet-support.

[17] T. Mironava, M. Hadjiargyrou, M. Simon, and M. H. Rafailovich, "The effects of UV emission from compact fluorescent light exposure on human dermal fibroblasts and keratinocytes in vitro," *Photochemistry and Photobiology*, vol. 88, no. 6, pp. 1497–1506, 2012.

[18] S. Li, "Hardware design guide to smartphone ambient-light sensing," *Electronic Design*. Accessed Jan. 10, 2020. [Online]. Available: https://www.electronicdesign.com/technologies/android/article/21801487/hardware-design-guide-to-smartphone-ambientlight-sensing.

[19] Adafruit, "RGB color sensor with IR filter and white LED – TCS34725." Accessed Sep. 18, 2019. [Online]. Available: https://www.adafruit.com/product/1334.

[20] Sparkfun, "SparkFun particle sensor breakout – MAX30105." Accessed Sep. 17, 2019. [Online]. Available: https://www.sparkfun.com/products/14045.

[21] C. Eskow, "Optical time of flight sensors: An overview," *EEworld Online*. Accessed Feb. 11, 2020. [Online]. Available: https://www.eeworldonline.com/optical-time-of-flight-sensors-an-overview/.

[22] A. AG, "Light-to-Frequency." Accessed Dec. 2, 2020. [Online]. Available: https://ams.com/light-to-frequency.

[23] "Vitamin D and your health: Breaking old rules, raising new hopes," *Harvard Men's Health Watch*. Accessed Feb. 11, 2020 [Online]. Available: https://www.health.harvard.edu/staying-healthy/vitamin-d-and-your-health-breaking-old-rules-raising-new-hopes.

[24] "Link Lab." University of Virginia Engineering." Accessed Feb. 15, 2020 [Online]. Available: https://engineering.virginia.edu/link-lab-0.

[25] D. Coley and J. Crabb, "An artificial intelligence approach to the prediction of natural lighting levels," *Building and environment*, vol. 32, no. 2, pp. 81–85, 1997.

[26] S. H. Begemann, A. D. Tenner, and G. J. Van Den Beld, "Lighting system for controlling the color temperature of artificial light under the influence of the daylight level," Feb. 24 1998. U.S. Patent 5,721,471.

[27] W. J. Fassbender, P. H. Mudge, and B. P. Platner, "Portable handheld artificial light detector," Jan. 5 2010. US Patent 7,642,501.

[28] F. Jazizadeh and J. Wang, "Artificial versus natural light source identification with light intensity sensors for energy monitoring," *Procedia Engineering*, vol. 145, pp. 956–963, 2016.

[29] Maxim Integrated, *MAX30105: High-Sensitivity Optical Sensor for Smoke Detection Applications*. Accessed Sep. 17, 2019. [Online]. Available: https://www.maximintegrated.com/en/products/interface/sensor-interface/MAX30105.html.

[30] TAOS: Texas Advanced Optoelectronics Solutions, TX, USA, *TCS3472 Color Light-to-Digital Converter with IR Filter*. Accessed Sep. 18, 2019. [Online]. Available: https://cdn-shop.adafruit.com/datasheets/TCS34725.pdf.

[31] "Tinycircuits." Accessed Sep. 12. 2019. [Online]. Available: https://tinycircuits.com/.

[32] Atmel Corporation, San Jose CA, USA, *ATmega328P: 8-bit AVR Microcontroller with 32K Bytes In-System Programmable Flash Datasheet*, 2015. Accessed Sep. 15. 2019. [Online]. Available: http://ww1.microchip.com/downloads/en/DeviceDoc/Atmel-7810-Automotive-Microcontrollers-ATmega328P_Datasheet.pdf.

[33] Nordic Semiconductor, *nRF51822 Multiprotocol Bluetooth low energy/2.4 GHz RF System on Chip*, 2014. Accessed Oct. 15, 2019. [Online]. Available: https://infocenter.nordicsemi.com/pdf/nRF51822_PS_v3.1.pdf.

[34] "Bluetooth smart: Introduction to bluetooth low energy." Accessed Jan. 26, 2020. [Online]. Available: https://learn.adafruit.com/introduction-to-bluetooth-low-energy?view=all.

[35] B. Kempke, P. Pannuto, B. Campbell, and P. Dutta, "Surepoint: Exploiting ultra wideband flooding and diversity to provide robust, scalable, high-fidelity indoor localization," in *Proceedings of the 14th ACM Conference on Embedded Network Sensor Systems CD-ROM*, pp. 137–149, 2016.

[36] L. Ada, *Downloads*. Adafruit. Accessed Nov. 20, 2019. [Online]. Available: https://learn.adafruit.com/adafruit-color-sensors/downloads.

[37] Fractus Antennas, *Micro Reach Xtend (FR05-S1-N-0-110) – Bluetooth, Zigbee, 802.11 b/g/n WLAN*, 2017. Accessed Nov. 15, 2019. [Online]. Available: https://www.fractusantennas.com/wp-content/uploads/2016/07/UM_FR05_S1_N_0_110.pdf.

[38] Maxim Integrated Products, Sunnyvale CA, USA, *MAXIM Low-dropout, 300mA Linear Regulators in SOT23*, 4th ed., 2009. Accessed Nov. 15, 2019. [Online]. Available: https://datasheets.maximintegrated.com/en/ds/MAX8887-MAX8888.pdf.

[39] University of California Berkeley, *nrf5x-base*. Accessed Oct. 28, 2019. [Online]. Available: https://github.com/lab11/nrf5x-base.

[40] STMicroelectronics, *BAL-NRF01D3 50 nominal input/conjugate match balun to nRF51422-QFAA, nRF24LE1, nRF51822-QFAA/AB, with integrated harmonic filter*, 7th ed., 2017.

[41] K. Townsend, *Adafruit TCS34725 Color Sensor Driver*. Adafruit. Accessed Nov. 17, 2019. [Online]. Available: https://github.com/adafruit/Adafruit_TCS34725.

[42] H. Palus, "Representations of colour images in different colour spaces," in *The Colour image processing handbook*, pp. 67–90, Springer, 1998.

[43] S. Chaudhuri, "Light and color," 2010. Stanford University. Accessed on Feb. 20, 2020. [Online]. Available: http://graphics.stanford.edu/courses/cs148-10-summer/docs/02_light_color.pdf.

[44] J. Hernandez-Andres, R. L. Lee, and J. Romero, "Calculating correlated color temperatures across the entire gamut of daylight and skylight chromaticities," *Applied optics*, vol. 38, no. 27, pp. 5703–5709, 1999.

[45] University of Central Arkansas, *Illumination and Distance*. Accessed on Feb. 2, 2020. [Online]. Available: https://faculty.uca.edu/njaustin/LabLibrary/LightLevels/brightness.pdf.

[46] J. Rowberg, *bglib: BGLib implementations for Bluegiga BLE112 Bluetooth Smart module*, 2017. Accessed on Jan. 15, 2020. [Online]. Available: https://github.com/jrowberg/bglib.

[47] I. Reda and A. Andreas, "Solar position algorithm for solar radiation applications," *Solar energy*, vol. 76, no. 5, pp. 577–589, 2004.